Babeș-Bolyai University
Faculty of Chemistry and Chemical Engineering
Supramolecular Organic and Organometallic
Chemistry Centre

COMPLEXES WITH LIGANDS WITH CHALCOGEN OR NITROGEN DONOR ATOMS. SYNTHESIS, STRUCTURAL CHARACTERIZATION, APPLICATIONS

Anamaria-Lavinia Rahovan (married Corjuc)

PhD thesis summary

Scientific advisor:
Prof. Dr. Anca Daniela Silvestru

Cluj-Napoca
2024

PhD committee

President: Prof. Dr. Niculina D. Hădade
"Babeș-Bolyai" University, Faculty of Chemistry and Chemical Engineering, Cluj-Napoca

Scientific advisor: Prof. Dr. Anca Daniela Silvestru
"Babeș-Bolyai" University, Faculty of Chemistry and Chemical Engineering, Cluj-Napoca

Reviewers: CSI Dr. Otilia Costișor
"Coriolan Drăgulescu" Institute of Chemistry of the Romanian Academy, Timișoara

Prof. Dr. Cecilia Cristea
"Iuliu Hațieganu" University of Medicine and Pharmacy, Faculty of Pharmacy, Cluj-Napoca

Conf. Dr. Ciprian I. Rat
"Babeș-Bolyai" University, Faculty of Chemistry and Chemical Engineering, Cluj-Napoca

Keywords: silver complexes, Sb(III) complexes, dinuclear Bi(III) compounds, ligands with chalcogen donor atoms, ligands with nitrogen donor atoms, hypercoordination, antiproliferative activity, luminescence, structural investigation.

Date of public defence: 28th of June, 2024

Content

I. INTRODUCTION.....1

II. SILVER COMPLEXES WITH LIGANDS HAVING GROUP 15 (N) OR 16 (S, Se) DONOR ATOMS.....3

II.1. Literature data…….3

II.2. Original contributions……...16

II.2.1. Ligands with chalcogen donor atoms and their silver complexes …..……16

II.2.1.1. Complexes of type [Ag(X){E($CH_2C_6H_4$Br-2)$_2$}] (X = OSO_2CF_3, ONO_2, $OClO_3$; E = S, Se)……..……16

II.2.1.2. Complexes of type [Ag(X){E($CH_2C_6H_4CH_3$-2)$_2$}] (X = OSO_2CF_3, ONO_2, $OClO_3$; E = S, Se)……..25

II.2.1.3. Complexes of type [Ag(X){E($CH_2C_6H_4$Y-2)$_2$}$_2$] (X = OSO_2CF_3, ONO_2, $OClO_3$; E = S, Se, Y = Br, CH_3)…….32

II.2.1.4. Antiproliferative activity assay……...……...….41

II.2.2. Ligands with nitrogen donor atoms and their silver complexes ……...……...…....42

II.3. Conclusions…….……..……...…51

III. COMPOUNDS OF GROUP 15 ELEMENTS (Sb, Bi)……...…….53

III.1. Literature data……...……...53

III.2. Original contributions……..…..…59

III.2.1. Bi(III) complexes ……...……...…..59

III.2.2. Sb(III) complexes ……...……..…….…..64

III.2.2.1. Reactions of [2-(Me_2NCH_2)C_6H_4SbO]$_3$ with carboxylic acids…….……..…….64

III.2.2.2. Reactions of [2-(Me_2NCH_2)C_6H_4SbO]$_3$ with trifluoromethanesulfonic acid and with pentafluophenol ……..…….…75

III.2.2.3. Reaction of [2-(Me_2NCH_2)C_6H_4SbO]$_3$ with tetraphenyldichalcogenoimidodiphosphinic acids.……..…….……..…..…79

III.3. Conclusions..……..……...……....…86

IV. EXPERIMENTAL DATA …….……..…88

IV.1. General data…….……...…….....…88

IV.2. Ligands with chalcogen donor atoms (S, Se) and their silver complexes……...…...89

IV.3. Ligands with nitrogen donor atoms and their silver complexes……....……...……..98

IV.4. Bi(III) complexes……...……...…….……...101

IV.5. Sb(III) complexes ……...……...…….…..103

V. BIBLIOGRAPHY……...…….…..109

VI. APPENDIX……...…….……..…115
LIST OF PUBLISHED PAPERS AND CONFERENCES...……136
ACKNOWLEDGEMENTS……...……...……...……...137

I. INTRODUCTION

Metal complexes today find a wide range of applications in various fields, such as organic synthesis (catalysts or transfer agents of organic groups), optoelectronics, magnetic materials, medicine, pharmaceuticals, etc. The specific activity of various chemical compounds is determined by the metal properties and/or of the ligands, as well as the nature and strength of the metal-ligand interactions.[1] As a result, in recent years there has been a particular interest in obtaining new ligands and, implicitly, new metal complexes, which ensure both the stability and the chemical reactivity necessary for the successful use of the latter in the mentioned fields.

Current studies are focused not only on increasing the efficiency of the complexes in terms of the specific activity, but also on reducing the costs, the sources of pollution and the toxicity of the obtained species, by using modern methods of synthesis and by replacing highly toxic metals with others that are friendly to the environment and the human body.

Transition metals in particular have proven to be active agents in catalytic processes (e.g. Pd, Pt, Ir, Ru),[2] but also in biological processes (Pt, Au, Ag)[3] or in optoelectronics (Au, Ag).[4,5] Main group metals (Sn, Sb, Bi) have been shown to be useful in obtaining nanomaterials and also in catalysis or in pharmaceutics and biology.[6–8] For a suitable design of such metal complexes, for a better control of their structure and properties when used for precise purposes, it is important to choose ligands capable to accommodate to the coordination sphere of the metal and having appropriate *hard/soft* properties.

The aim of this work was to obtain metal complexes with ligands with chalcogen or nitrogen donor atoms. Considering the antibacterial or the antitumor properties of silver and its compounds, as well as the *soft* character of this metal, a series of ligands with *soft* donor atoms, respective sulphur or selenium (**L1**-**L4**), as well as silver(I) complexes (**1**-**18**) with S→Ag or Se→Ag interactions were prepared. Two ligands (**L7**-**L8**) with nitrogen donor atoms were also synthetised, as well as their complexes (**19**-**20**) with N→Ag interactions. The structural investigation of the new complexes occupies an important place in the studies carried out, considering the relationship structure – chemical reactivity – specific properties. Some of the obtained silver complexes (**8**, **11**, **15** and **16**), were tested as antitumor agents, while for complexes **2**, **5** and the ligands **L1**, **L2** the luminescent properties were evaluated.

Ligands with oxygen atom donors, respectively carboxylic acids, phenols and tetraphenyldioxoimidodiphosphinic acid, were used to obtain some organoantimony(III) complexes, stabilized by the organic group 2-(Me_2NCH_2)C_6H_4. Such aryl groups with pendant

arms capable of intramolecular N→Sb coordination led to the stabilization of the respective species by hypercoordination.[9] The preparation of such complexes had in mind the evaluation of the chemical reactivity of the cyclic trimers $[2\text{-}(Me_2NCH_2)C_6H_4SbO]_3$, as well as the structural particularities determined by the used ligands (**25**-**33**). Considering the *hard* character of group 15 metals, the behaviour of antimony was followed in the presence of *soft* donors also, respectively tetraphenyldithio- or tetraphenylmonothioimidodiphosphinic ligands (**34**-**36**).

In order to extend the studies on the reactivity of some organometallic compounds of group 15 elements, recourse was made to the synthesis of some dinuclear Bi(III) compounds (**21**-**24**), stabilized by intramolecular N→Bi coordination, and containing Bi–E–Bi (E = O, S, Se, Te) fragments.

II.2. Original contributions

II.2.1. Ligands with chalcogen donor atoms and their silver complexes

II.2.1.1. Complexes of type [Ag(X){E(CH$_2$C$_6$H$_4$Br-2)$_2$}] (X = OSO$_2$CF$_3$, ONO$_2$, OClO$_3$; E = S, Se)

New silver complexes with ligands of type (2-BrC$_6$H$_4$CH$_2$)$_2$E [E = S (**L1**), Se(**L2**)] were synthetised, in absence of light, according to the reactions depicted in **Scheme 1**. After reactions between ligands and various silver salts, such as silver nitrate, silver triflate and silver perchlorate, new complexes were obtained. The ligand **L1**[65] was already reported in the literature and during these studies the same method as that described previously was used. The Se analogue is not known, and it was obtained in the reaction between 2-bromobenzyl bromide and Na$_2$Se freshly prepared.[66]

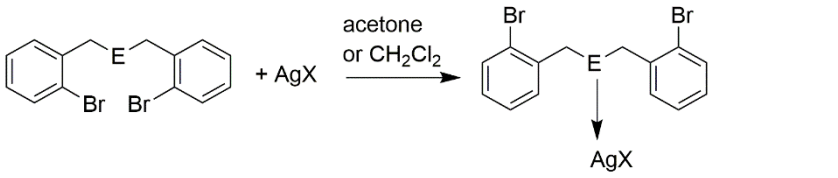

Scheme 1

The complexes were investigated by NMR spectroscopy, IR spectroscopy, mass spectrometry, and for some of them the molecular structure was determined by single crystal X-ray diffraction. The ^{1}H NMR spectra for the ligand (2-BrC$_6$H$_4$CH$_2$)$_2$S (**L1**) and complexes **1** and **2** are presented in **Figure 1**.

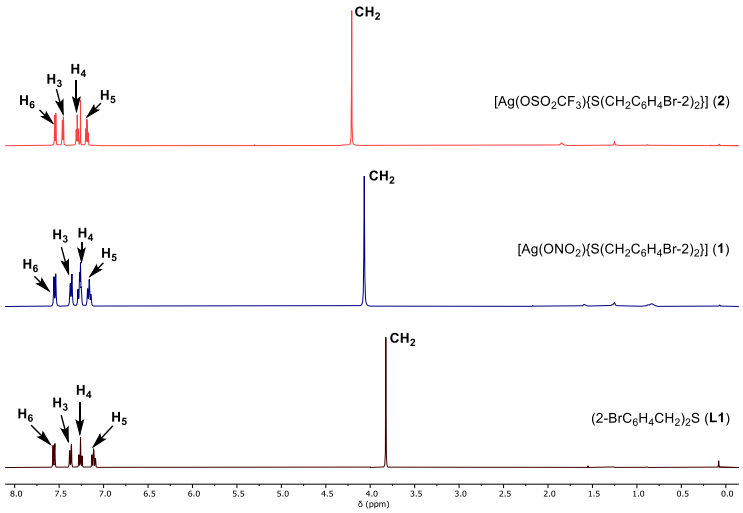

Figure 1. ^{1}H NMR spectra (CDCl$_3$, 400.13 MHz) for complexes **1**, **2** and the ligand (2-BrC$_6$H$_4$CH$_2$)$_2$S (**L1**).

In the ESI+ mass spectra of complexes **1-12** the molecular ions were not identified. The base peak identified to all complexes correspond to the $[AgL]^+$ cation. The ESI+ mass spectra of complexes **1-12** were recorded in methanol, with exception of the complexes **3** and **6**, for which were recorded in a mixture of dimethyl sulfoxide and methanol.

Although the ligand $(2\text{-}BrC_6H_4CH_2)_2S$ (**L1**) was previously reported in literature,[65] the molecular structure was not determined. In our case we managed to isolate single crystals for both ligands and they were investigated by X-ray diffraction (**Figure 2**). Single crystals were obtained from hexane for the ligand $(2\text{-}BrC_6H_4CH_2)_2Se$ (**L2**).

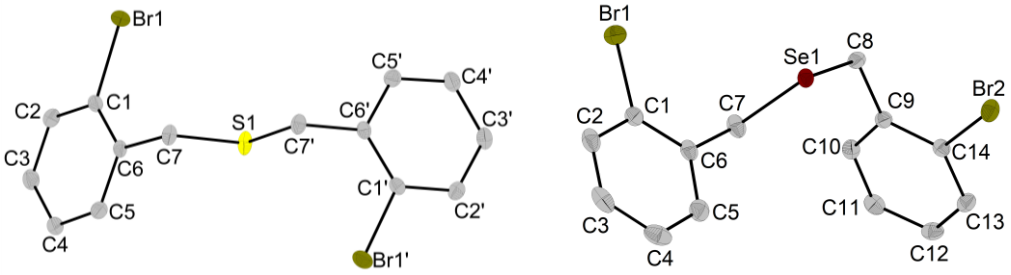

(a) (b)

Figure 2. Thermal ellipsoids representation at 50% probability of the molecular structures of $(2\text{-}BrC_6H_4CH_2)_2S$ (**L1**) (a) and $(2\text{-}BrC_6H_4CH_2)_2Se$ (**L2**) (b). Hydrogen atoms were omitted for clarity.

The ligand **L1** crystalized in the orthorhombic system, space group P 21 21 2, and the ligand **L2** crystalized in the triclinic system P-1. In case of the diorganoselenide **L2** were observed hydrogen···selenium intermolecular interactions (**Figure 3**), which led to the formation of polymeric chains through Se1···H3 contacts (3.065(2) Å) and Se1···H11 (3.039(2) Å). These interactions are close to the sum of the van der Waals radii (3.20 Å) of the two elements.[67]

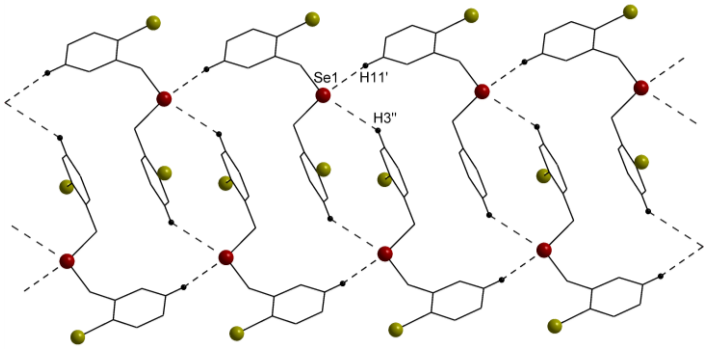

Figure 3. Association by H···Se interactions in the ligand $(2\text{-}BrC_6H_4CH_2)_2Se$ (**L2**) [symmetry operation: *x, 1+y, z* (′); *-x, 2-y, 1-z* (′′)]. Hydrogen atoms which are not involved in interactions were omitted for clarity.

The molecular structures of complexes **2** and **5** were also determined by single crystal X-ray diffraction. In each compound was observed that the ligand is bonded to the silver atom through chalcogen-silver interactions (S→Ag 2.4732(4) Å and Se→Ag 2.5480(3) Å).

The OSO_2CF_3 ligand behaves as a triconnective bidentate moiety in complex **2**, and as a biconnective monodentate moiety in complex **5**, thus resulting in dimeric associations (**Figure 4**).

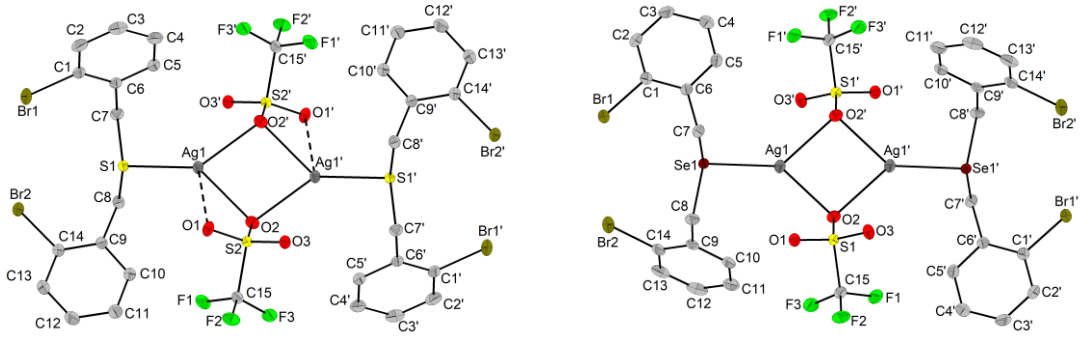

(a) (b)

Figure 4. Thermal ellipsoids representation at 50% probability for the dimers $[Ag(OSO_2CF_3)\{S(CH_2C_6H_4Br\text{-}2)_2\}]$ (**2**) (a) [symmetry operation: *1-x, 1-y, 1-z* (′)] and $[Ag(OSO_2CF_3)\{Se(CH_2C_6H_4Br\text{-}2)_2\}]$ (**5**) (b) [symmetry operation : *1-x, 1-y, 1-z* (′)].

The optical properties for both ligands and their silver triflate complexes were measured in 10^{-6} M CH_2Cl_2 solutions. The recorded spectra showed that both the ligands and their complexes present luminescence (**Figure 5**).

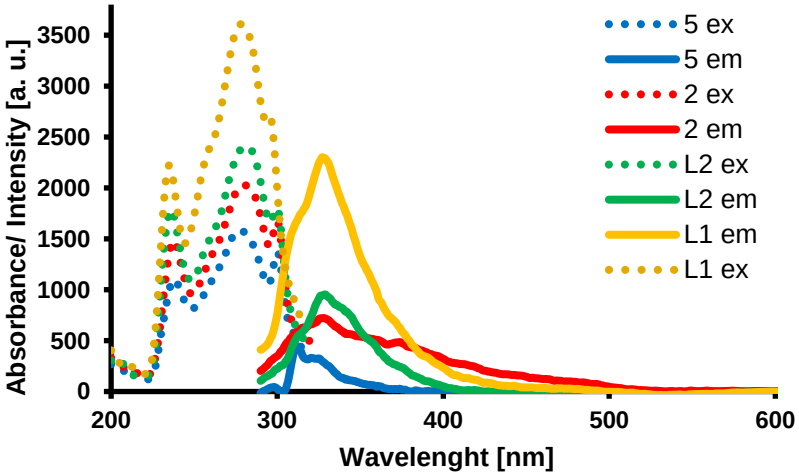

Figure 5. Luminescence spectra for ligands $(2\text{-}BrC_6H_4CH_2)_2E$ (E = S (**L1**), Se (**L2**)) and complexes **2** and **5**.

The excitation bands with maximum intensity were observed at ν (nm) 280 (**5**), 280 (**2**), 325 (**L2**), 388 (**L1**), and the emission bands with maximum intensity were observed at ν (nm) 330 (**5**), 330 (**2**), 254 (**L2**), 295 (**L1**) value.

The molar conductivity (**Table 1**) for the silver complexes and both ligands were determined in freshly prepared methanol solutions with a concentration of 10^{-3} M. In the case of complexes **1**-**6**, it was observed that they are completely dissociated in solution (Λ_M in the range 111.8-155.2)[68,69] and their behaviour corresponds to 1 : 1 electrolytes, which contain the $[AgL]^+$ cation and an X^- anion.

Table 1. The molar conductivity of the ligands **L1**, **L2** and the complexes **1**-**6** (10^{-3} M solutions in MeOH, 20 ºC).

	Complexes	Λ_M ($\Omega^{-1}\cdot cm^2\cdot mol^{-1}$)
L1	$(2\text{-}BrC_6H_4CH_2)_2S$	1.83
L2	$(2\text{-}BrC_6H_4CH_2)_2Se$	14.14
1	$[Ag(ONO_2)\{S(CH_2C_6H_4Br\text{-}2)_2\}]$	111.8
2	$[Ag(OSO_2CF_3)\{S(CH_2C_6H_4Br\text{-}2)_2\}]$	135.4
3	$[Ag(OClO_3)\{S(CH_2C_6H_4Br\text{-}2)_2\}]$	155.2
4	$[Ag(ONO_2)\{Se(CH_2C_6H_4Br\text{-}2)_2\}]$	105.8
5	$[Ag(OSO_2CF_3)\{Se(CH_2C_6H_4Br\text{-}2)_2\}]$	120.4
6	$[Ag(OClO_3)\{Se(CH_2C_6H_4Br\text{-}2)_2\}]$	144.9

II.2.1.2. Complexes of type $[Ag(X)\{E(CH_2C_6H_4CH_3\text{-}2)_2\}]$ (X = OSO_2CF_3, ONO_2, $OClO_3$; E = S, Se)

As a continuation of the previous studies, we investigated the changes in the electronic environment provided by the use of the organic group $2\text{-}CH_3C_6H_4CH_2$. The ligands $(2\text{-}CH_3C_6H_4CH_2)_2E$ (E = S (**L3**), Se (**L4**)) were reported previously,[70,71] but they were prepared during these studies by another procedure, namely the same one used to obtain the ligands substituted with bromine at the aromatic nucleus. The ligand **L3** was previously characterized only in solution. During the studies carried out in this work, by recrystallization from pentane, suitable single crystals for determination of the molecular structure by X-ray diffraction could be obtained (**Figure 6**). The coordination geometry around the sulphur atom is Ψ-tetrahedral.

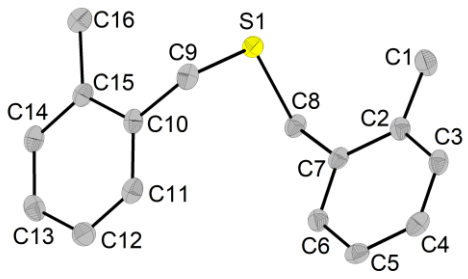

Figure 6. Thermal ellipsoids representation at 30% probability of the molecular structure of $(2\text{-}CH_3C_6H_4CH_2)_2S$ (**L3**). Hydrogen atoms were omitted for clarity.

Using the same Ag salts as for the ligands substituted with bromine at the aromatic core, other six complexes were obtained (**Scheme 2**). The complexes were structurally investigated, both in solution and in solid state.

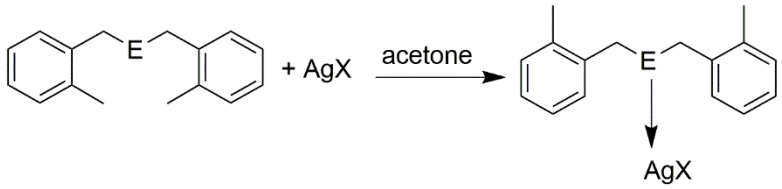

E = S: X = NO_3 (**7**), OTf (**8**), ClO_4 (**9**)
E = Se: X = NO_3 (**10**), OTf (**11**), ClO_4 (**12**)

Scheme 2

The $^{77}Se\{^1H\}$ NMR spectra show characteristic singlet resonance signals for the Se atom in each complex (**Figure 7**). The value of the chemical shift for the ligand is δ = 262.9 ppm, and the values for complexes **10** (δ 226.6 ppm) and **11** (δ 225.2 ppm) are quite close each other.

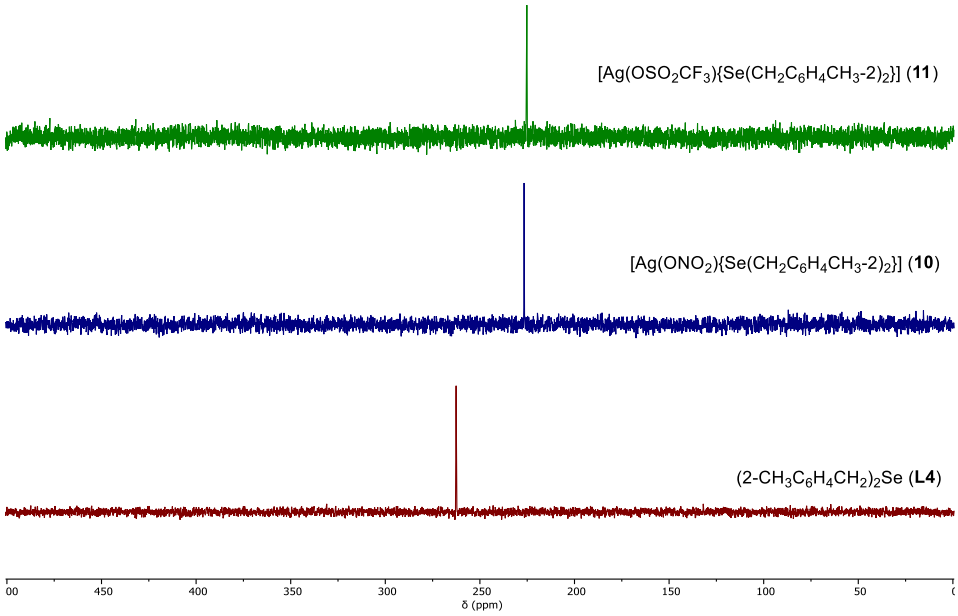

Figure 7. $^{77}Se\{^1H\}$ NMR spectra ($CDCl_3$, 76.33 MHz) for complexes **10**, **11** and the ligand (2-$CH_3C_6H_4CH_2)_2Se$ (**L4**).

Complexes **1**-**12** were also characterized by infrared spectroscopy. In the IR spectrum of complex **7** (**Figure 8** (**a**)) intense bands were observed around 1454, 1281 and 1022 cm^{-1}. These values suggest that the NO_3^- ligand is coordinated in a bidentate fashion to silver.

The triflato ligand behaves as a monodentate ligand in all complexes. In the IR spectrum of compound **8** (**Figure 8** (**b**)) intense bands were observed at 1211, 1172, 1150 and 1016 cm^{-1}, which suggest that the triflato ligand is coordinated in a monodentate fashion to the Ag atom.

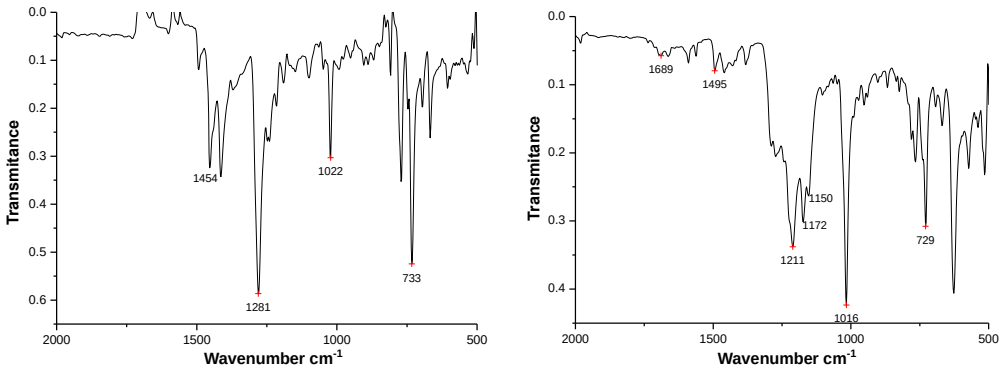

(a) (b)

Figure 8. ATR spectra of the complexes $[Ag(ONO_2)\{S(CH_2C_6H_4CH_3\text{-}2)_2\}]$ (**7**) (a) and $[Ag(OSO_2CF_3)\{S(CH_2C_6H_4CH_3\text{-}2)_2\}]$ (**8**) (b).

In the molecular structures of the complexes **7** and **10** (**Figure 9**) can be observed strong interactions between the chalcogen and the Ag atom (Ag1–S1 2.4709(4) Å and Ag1–Se1 2.5462(3) Å). The coordination geometry around the silvers atoms is a distorted trigonal pyramid, where the metal atom is positioned on the top of the pyramid at 0.43 Å above the S1O1O3 plane in **7** and at 0.26 Å above the plane Se1O1O3 in **10**.

Both complexes **7** and **10**, are crystalized in the monoclinic P 21/c space group. The nitrato ligand is coordinated in a bidentate fashion to Ag in both compounds. In complex **7** the secondary interaction Ag···O (2.8184(4) Å) is stronger than in complexes **10** (3.0969(1) Å).

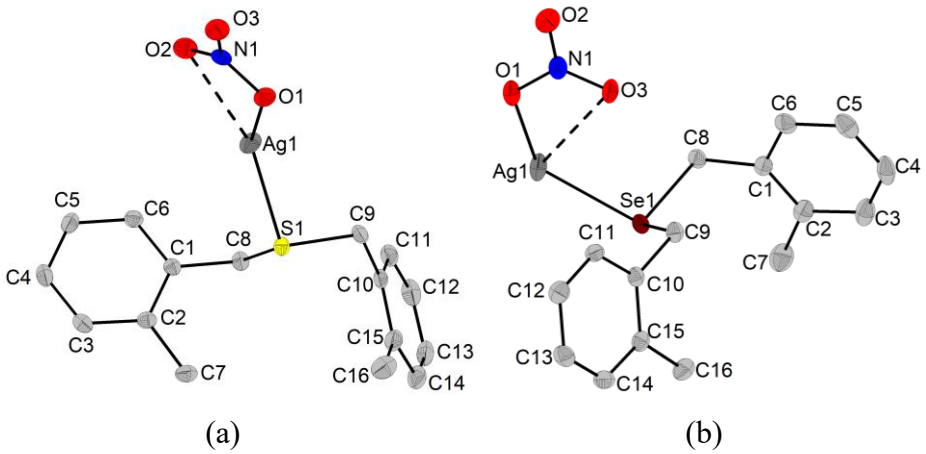

(a) (b)

Figure 9. Thermal ellipsoids representation at 50% probability of the molecular structures of $[Ag(ONO_2)\{S(CH_2C_6H_4CH_3\text{-}2)_2\}]$ (**7**) (a) and $[Ag(ONO_2)\{Se(CH_2C_6H_4CH_3\text{-}2)_2\}]$ (**10**) (b). Hydrogens atoms were omitted for clarity.

II.2.1.3. Complexes of type $[Ag(X)\{E(CH_2C_6H_4Y\text{-}2)_2\}_2]$ (X = OSO_2CF_3, ONO_2, $OClO_3$; E = S, Se; Y = Br, CH_3)

After changing the molar ratio ligand : metal 1 : 1 with a molar ratio 2 : 1, six new complexes were obtained, namely $[Ag(ONO_2)\{S(CH_2C_6H_4Br\text{-}2)_2\}_2]$ (**13**), $[Ag(ONO_2)\{Se(CH_2C_6H_4Br\text{-}2)_2\}_2]$ (**14**), $[Ag(ONO_2)\{Se(CH_2C_6H_4CH_3\text{-}2)_2\}_2]$ (**15**), $[Ag(OSO_2CF_3)\{Se(CH_2C_6H_4CH_3\text{-}2)_2\}_2]$ (**16**), $[Ag(OClO_3)\{S(CH_2C_6H_4CH_3\text{-}2)_2\}_2]$ (**17**) and $[Ag(OClO_3)\{Se(CH_2C_6H_4CH_3\text{-}2)_2\}_2]$ (**18**), where two ligands are coordinated to each silver atom. In **Scheme 3** are represented the syntheses of the silver complexes with a 2 : 1 L : Ag molar ratio.

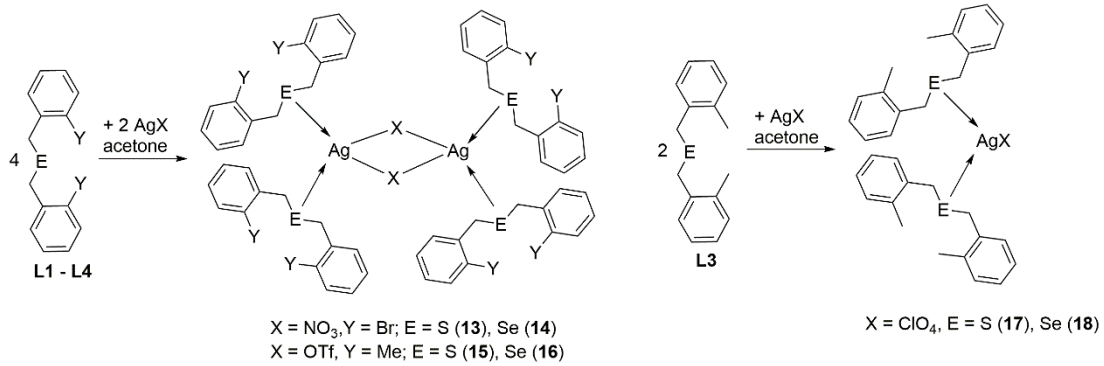

Scheme 3

Single crystals of compound **14** (monoclinic system, space group P 21/n) were obtained by slow solvent evaporation from a solution in MeOH. The formation of dimeric associations based on bridging nitrato ligands was observed by single crystal X-ray diffraction (**Figure 10**). The two diorganoselenolato ligands are coordinated to the Ag atom by selenium. The nitrato ligand acts as a bimetallic bioconvective moiety in a κ^2O1O2-μ-O1(Ag, Ag) fashion. The coordination geometry around both silver atoms is distorted (τ_5 = 0.25), intermediate between a square pyramid (τ_5 = 0) and a trigonal bipyramid (τ_5 = 1).[73] The two oxygen atoms and the two silver atoms form a planar Ag_2O_2 cycle. The interatomic distances between the oxygen atoms and silver have close values (Ag1–O1 2.351(3) Å, Ag1–O1′ 2.482(3) Å).

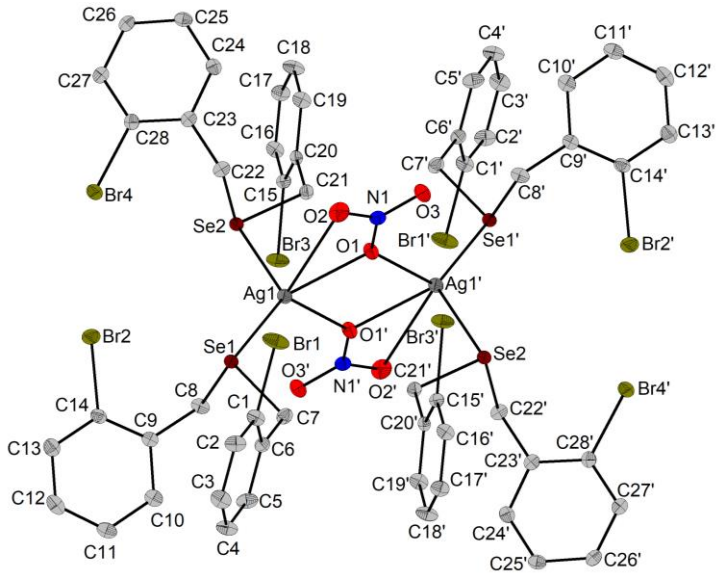

Figure 10. Thermal ellipsoids representation at 30% probability of a dimer in the compound crystal $[Ag(ONO_2)\{Se(CH_2C_6H_4Br\text{-}2)_2\}_2]$ (**14**). [symmetry operations: *1-x, 1-y, 1-z* (′)]**.** Hydrogen atoms were omitted for clarity.

In the molecular structures of the complexes **15** and **16** is observed that two ligands are bonded to the same silver atom through the sulphur and the selenium donor atoms, respectively. In both structures can be observed that in the crystals are established Ag1···O2 [3.746(2) Å (**15**), (3.155(5) Å (**16**)] secondary interactions with values within the range between the sum of the covalent radii and the sum of the van der Waals radii for the two elements (Σr_{cov}(Ag,O) 2.11 Å, Σr_{vdW}(Ag,O) 4.09 Å).[67] Considering that the OSO_2CF_3 ligand acts bidentate, the silver atoms become tetracoordinated and the geometry is intermediate between see-saw (τ_4 = 0.43), and tetrahedral (τ_4 = 1.00),[74] the calculated τ_4 value being 0.75 for the complex **15** and 0.65 for the complex **16**. It was observed that both complex **15** and complex **16** form dimeric associations (**Figure 11**).

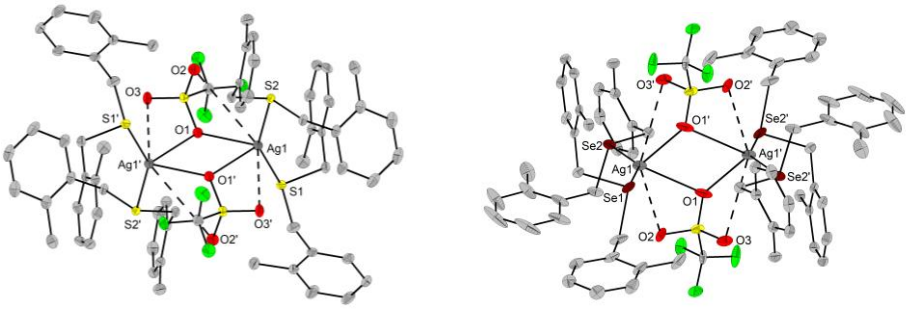

(a) (b)

Figure 11. Thermal ellipsoids representation at 30% probability of the dimeric structures in $[Ag(OSO_2CF_3)\{S(CH_2C_6H_4CH_3\text{-}2)_2\}_2]$ (**15**) (a) [symmetry operation: *1-x, 1-y, 1-z* (′)] and $[Ag(OSO_2CF_3)\{Se(CH_2C_6H_4CH_3\text{-}2)_2\}_2]$ (**16**) (b) [symmetry operation: *2-x, 1-y, 1-z* (′)]. Hydrogen atoms were omitted for clarity.

The unit cell in complexes **17** contains two independent molecules, between which Ag···Cg and O···H interactions are established (Ag1···Cg(C33-C38) 2.958(4) Å and O4···H35 2.538(6) Å). Each independent molecule contains two ligands and a perchlorate group (**Figure 12**). The coordination geometry around the Ag1 atom is a distorted trigonal pyramid with Ag1 placed inside the pyramid at 0.64 Å above the O1S1S2 plane and Cg placed at the top of the pyramid, while the Ag2 atom is positioned at the top of the pyramid having the base S3S4O5.

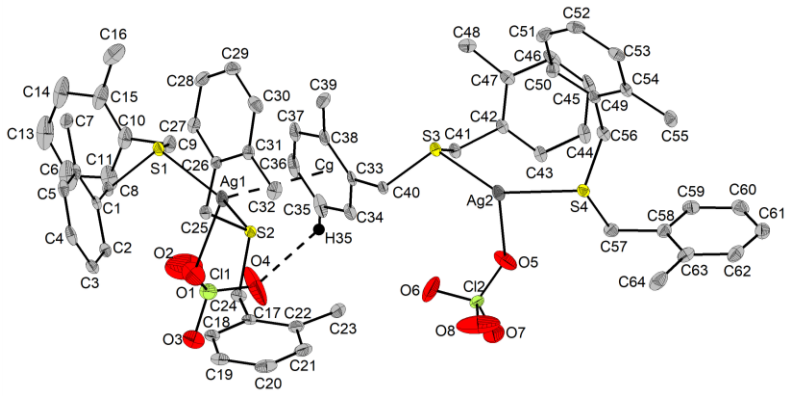

Figure 12. Thermal ellipsoids representation at 30% probability of the two independent molecules (**17a** and **17b**) in $[Ag(OClO_3)\{S(CH_2C_6H_4CH_3\text{-}2)_2\}_2]$ (**17**). Hydrogen atoms not involved in interactions were omitted for clarity.

II.2.1.4. Antiproliferative activity assay

The complexes **8**, **11**, **15** and **16** were tested for their antiproliferative activity against B16.F10 murine melanoma cells, using a colorimetric assay ELISA-BrdU. In **Figure 13** it is represented the effect of the silver complexes on the proliferation of the cancer cells, taking into account the influence of the concentration of the compounds used.

The complexes **8**, **11**, **15** and **16** present toxicity towards the B16.F10 cells. The IC_{50} values for these complexes indicate a very good activity in comparison with the standard Dacarbazine,[75] as can be seen from the data in **Table 2**.

Table 2. Antiproliferative effect of compounds **8**, **11**, **15** and **16** towards B16.F10 murine melanoma cells.

Compounds	**8**	**11**	**15**	**16**	Dacarbazina[75]
IC_{50} (μM)	28.72	36.97	25.35	32.41	149.7

Practically the tested complexes have a similar antiproliferative activity, comparable to that of silver triflate (IC_{50} = 29.34),[53] but the ligands showed no antiproliferative activity.

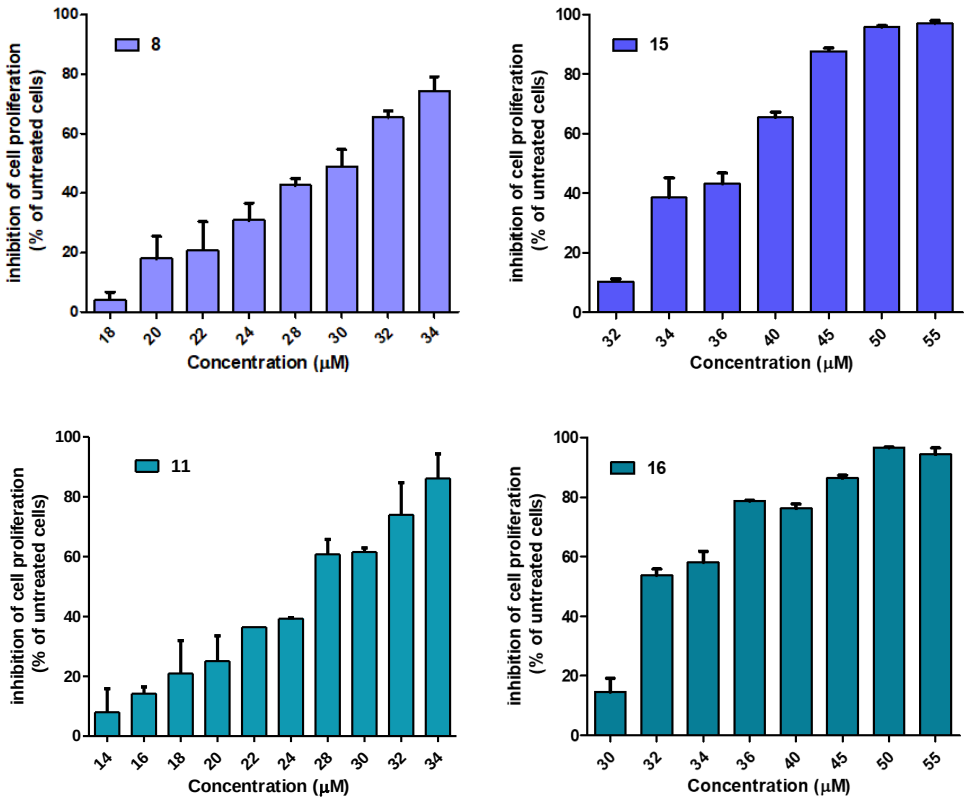

Figure 13. Concentration-dependent antiproliferative effect of complexes $[Ag(OSO_2CF_3)\{S(CH_2C_6H_4CH_3\text{-}2)_2\}]$ (**8**), $[Ag(OSO_2CF_3)\{Se(CH_2C_6H_4CH_3\text{-}2)_2\}]$ (**11**), $[Ag(OSO_2CF_3)\{S(CH_2C_6H_4CH_3\text{-}2)_2\}_2]$ (**15**) and $[Ag(OSO_2CF_3)\{Se(CH_2C_6H_4CH_3\text{-}2)_2\}_2]$ (**16**) in comparison with untreated control B16.F10 murine melanoma cells.

II.2.2. Ligands with nitrogen donor atoms and their silver complexes

Another type of ligands synthetized during these studies were those with nitrogen donor atoms. The ligands **L5-L8** were obtained starting from 2-bromobenzyl bromide. In **Scheme 4** are represent the reactions used for the preparation of ligands **L5-L8**.

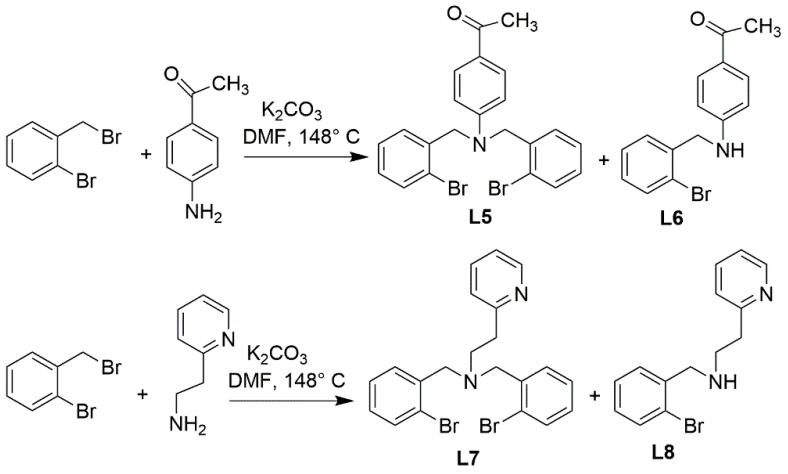

Scheme 4

In **Figure 14** are presented the ^{1}H NMR spectra for compounds **L5** and **L6**, as well as the spectrum of the mixture **L5**+**L6**.

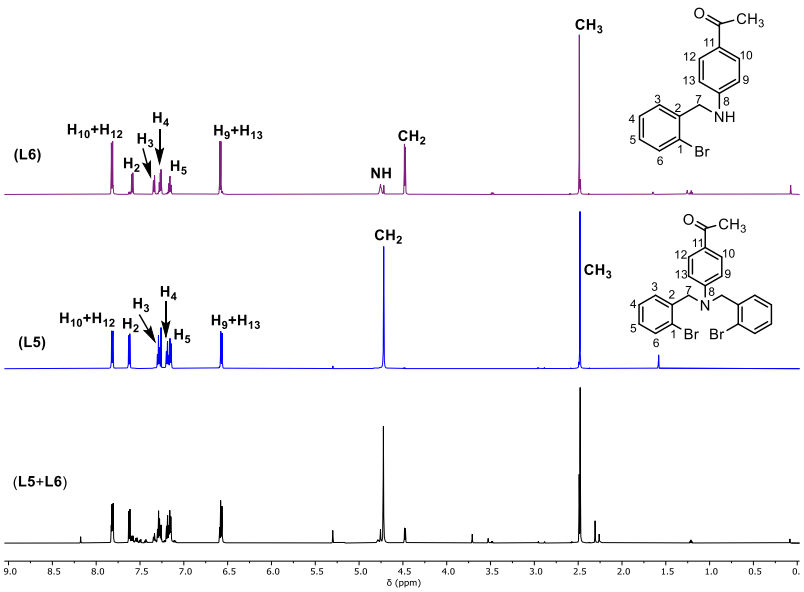

Figure 14. ^{1}H NMR spectra ($CDCl_3$, 600.13 MHz) of the mixture **L5**+**L6** and of the ligands **L5** and **L6**.

The molecular structure of the ligand **L5** (**Figure 15**) was determined by single crystal X-ray diffraction.

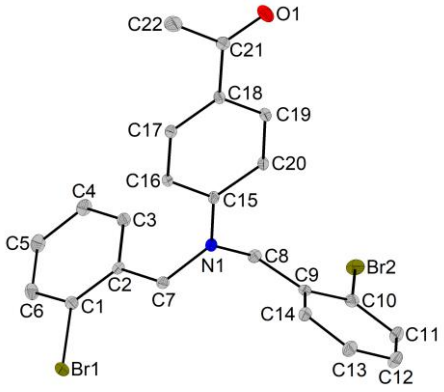

Figure 15. Thermal ellipsoids representation at 30% probability of the molecular structure of $CH_3C(O)C_6H_4N(CH_2C_6H_4Br\text{-}2)_2$ (**L5**). Hydrogen atoms were omitted for clarity.

After reacting 2-bromobenzyl bromide and 2-(2-aminoethyl) pyridine, similarly with the situation observed for **L5** and **L6**, a mixture which contains **L7** and **L8** was obtained, although an excess of 2-bromobenzyl bromide was used (molar ratio 3 : 1). The compounds were separated by column chromatography, by using silica gel as filler and a Et_2O/MeCN (1 : 1, v/v) mixture as eluent for the separation of **L7**, and methanol for the separation of **L8**. Both compounds were obtained as oils.

The ligand **L7** was reacted with silver salts (molar ratio 1 : 1) in order to obtain complexes **19**-**20** (**Scheme 5**).

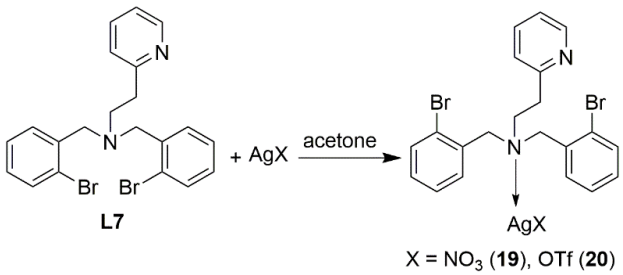

Scheme 5

The $^{13}C\{^{1}H\}$ NMR spectra of the complexes **20** is represented in **Figure 16**.

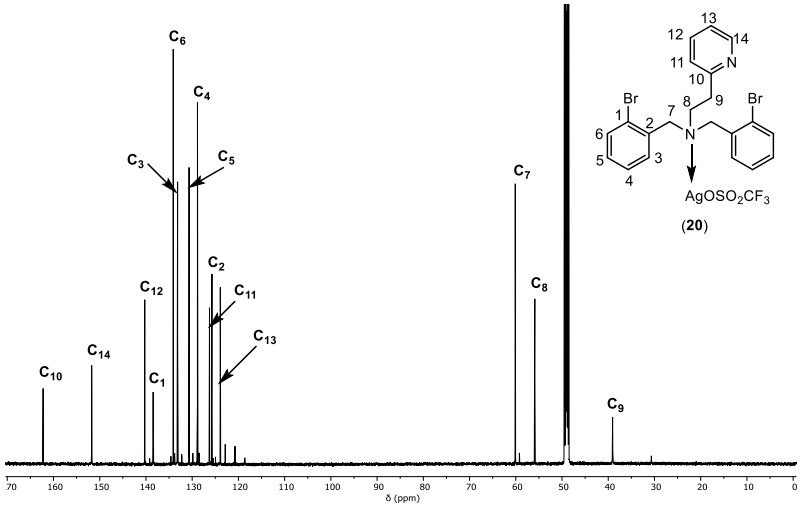

Figure 16. $^{13}C\{^{1}H\}$ NMR spectrum (methanol-d_4, 150.92 MHz) of the complexes $[Ag(OSO_2CF_3)\{PyCH_2CH_2N(CH_2C_6H_4Br\text{-}2)_2\}]$ (**20**).

The molecular structure of the complex **19** revealed that the ligand **L7** behaves in a bidentate fashion, bridging two neighbouring silver atoms. The dimers thus formed are associated in a three-dimensional network (**Figure 17**).

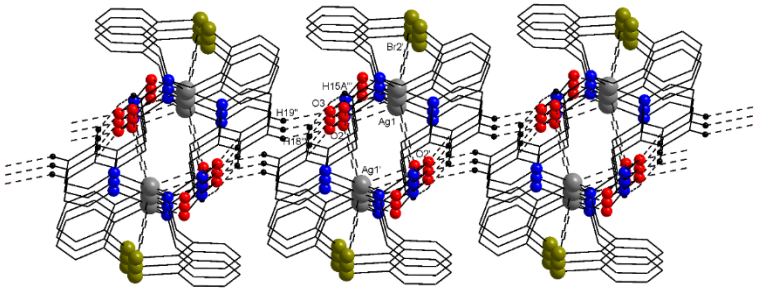

Figure 17. 3D supramolecular structure in the compound $[Ag(ONO_2)\{PyCH_2CH_2N(CH_2C_6H_4Br\text{-}2)_2\}]_2$ (**19**) [symmetry operation: *1-x, 1-y, 1-z* ('); *x, -1+y, z* (''); *2-x, 1-y, 1-*z (''')]. Hydrogen atoms which not involved in intermolecular interactions were omitted for clarity.

II.3. Conclusions

Eight ligands were synthetized, four with chalcogen donor atoms and four with nitrogen donor atoms, as followings: $(2\text{-}BrC_6H_4CH_2)_2E$ [E = S (**L1**), Se (**L2**)], $(2\text{-}CH_3C_6H_4CH_2)_2E$ [E = S (**L3**), Se (**L4**)], $CH_3C(O)C_6H_4N(CH_2C_6H_4Br\text{-}2)_2$ (**L5**), $CH_3C(O)C_6H_4N(H)(CH_2C_6H_4Br\text{-}2)$ (**L6**), $PyCH_2CH_2N(CH_2C_6H_4Br\text{-}2)_2$ (**L7**), $PyCH_2CH_2N(H)(CH_2C_6H_4Br\text{-}2)$ (**L8**). Five of them are new compounds (**L2**, **L5**, **L6**, **L7**, **L8**), first time reported in this thesis.

For the ligands $(2\text{-}BrC_6H_4CH_2)_2E$ [E = S (**L1**), Se(**L2**)], $(2\text{-}CH_3C_6H_4CH_2)_2E$ [E = S (**L3**), Se (**L4**)], $CH_3C(O)C_6H_4N(CH_2C_6H_4Br\text{-}2)_2$ (**L5**) the molecular and crystal structures were determined by single crystal X-ray diffraction. The ligands **L1**, **L2** and **L3** show the same coordination geometry around the chalcogen atoms, which is Ψ-tetrahedral. In the ligands **L2** and **L5** there are intermolecular interactions which led to the formation of a polymeric chain in the first, and a 3D supramolecular network in the second.

The reactions between the ligands **L1**, **L2**, **L3**, **L4** and silver salts ($AgNO_3$, AgOTf, $AgClO_4$) led to the formation of eighteen new complexes. Complexes **1**-**12** were obtained using a 1 : 1 molar ratio, and complexes **13**-**18** were obtained using a 2 : 1 molar ratio. In all complexes the ligands coordinate to the metal through the chalcogen atom.

Complexes $[Ag(OSO_2CF_3)\{S(CH_2C_6H_4Br\text{-}2)_2\}]$ (**2**), $[Ag(OSO_2CF_3)\{Se(CH_2C_6H_4Br\text{-}2)_2\}]$ (**5**), $[Ag(ONO_2)\{S(CH_2C_6H_4CH_3\text{-}2)_2\}]$ (**7**), $[Ag(ONO_2)\{Se(CH_2C_6H_4CH_3\text{-}2)_2\}]$ (**10**), $[Ag(ONO_2)\{Se(CH_2C_6H_4Br\text{-}2)_2\}_2]$ (**14**), $[Ag(OSO_2CF_3)\{S(CH_2C_6H_4CH_3\text{-}2)_2\}_2]$ (**15**), $[Ag(OSO_2CF_3)\{Se(CH_2C_6H_4CH_3\text{-}2)_2\}_2]$ (**16**) and $[Ag(OClO_3)\{S(CH_2C_6H_4CH_3\text{-}2)_2\}_2]$ (**17**) were characterized in solid state by single crystal X-ray diffraction, and the complexation through strong chalcogen-silver interactions was highlighted.

In the crystals of the complexes $[Ag(OSO_2CF_3)\{S(CH_2C_6H_4Br\text{-}2)_2\}]$ (**2**), $[Ag(OSO_2CF_3)\{Se(CH_2C_6H_4Br\text{-}2)_2\}]$ (**5**) $[Ag(ONO_2)\{Se(CH_2C_6H_4Br\text{-}2)_2\}_2]$ (**14**), $[Ag(OSO_2CF_3)\{S(CH_2C_6H_4CH_3\text{-}2)_2\}_2]$ (**15**) and $[Ag(OSO_2CF_3)\{Se(CH_2C_6H_4CH_3\text{-}2)_2\}_2]$ (**16**) the molecules form dimeric associations by means of oxygen atoms from the triflate or nitrate groups, which are involved in bridging two neighbouring Ag atoms. Complexes $[Ag(ONO_2)\{S(CH_2C_6H_4CH_3\text{-}2)_2\}]$ (**7**) and $[Ag(ONO_2)\{Se(CH_2C_6H_4CH_3\text{-}2)_2\}]$ (**10**) form one-dimensional coordination polymers by means of nitrato ligands.

In solution, complexes **1**-**18** are totally dissociated, thus corresponding to 1 : 1 electrolytes which contain the cation $[AgL]^+$ or $[AgL_2]^+$, and the anion X^-.

Ligands (2-$BrC_6H_4CH_2)_2E$ (E = S (**L1**), Se (**L2**)), as well as the complexes **2** and **5** have luminescente properties.

Complexes $[Ag(OSO_2CF_3)\{S(CH_2C_6H_4CH_3\text{-}2)_2\}]$ (**8**), $[Ag(OSO_2CF_3)\{Se(CH_2C_6H_4CH_3\text{-}2)_2\}]$ (**11**), $[Ag(OSO_2CF_3)\{S(CH_2C_6H_4CH_3\text{-}2)_2\}_2]$ (**15**) and $[Ag(OSO_2CF_3)\{Se(CH_2C_6H_4CH_3\text{-}2)_2\}_2]$ (**16**) were tested for their antitumoral potential and they showed a better antiproliferative activity against the B16.F10 murine melanoma cells than the standard used (dacarbazine). In contrast, ligands **L1**-**L4** did not show cytotoxicity up to 300 μM concentration.

The reactions between the ligand $PyCH_2CH_2N(CH_2C_6H_4Br\text{-}2)_2$ (**L7**) and silver salts ($AgNO_3$, AgOTf) in a 1 : 1 molar ratio led to the formation of two new complexes, namely $[Ag(ONO_2)\{PyCH_2CH_2N(CH_2C_6H_4Br\text{-}2)_2\}]$ (**19**) and $[Ag(OSO_2CF_3)\{PyCH_2CH_2N(CH_2C_6H_4Br\text{-}2)_2\}]$ (**20**). Their characterization was performed in solution by ^{1}H, ^{13}C, ^{19}F NMR spectroscopy and by APCI+ mass spectrometry. For the complex **19**, the solid state structure was determined by single crystal X-ray diffraction, emphasizing the formation of dimeric associations through bridging organic ligands.

III. COMPOUNDS OF GROUP 15 ELEMENTS (Sb, Bi)

III.1. Literature data

III.2. Original contributions

III.2.1. Bi(III) complexes

The synthesis of dinuclear diorganobismuth(III) compounds, with *C,N,C*-Bi fragments and a butterfly type skeleton, is shown in **Scheme 6**. Compounds **21**-**24** were obtained in the reaction between diorganobismuth(III) bromide and the appropriate sodium chalcogenide or NaOH. Sodium selenide and sodium telluride was freshly preparate in the rection between selenium or tellurium powder and sodium borohydride, according to the method described in the literature.[66]

The dinuclear compound **24** was obtained in mixture with another compound, which, according to the ^{125}Te NMR spectrum, was assigned to a species containing a $R_2Te{=}O$ fragment.

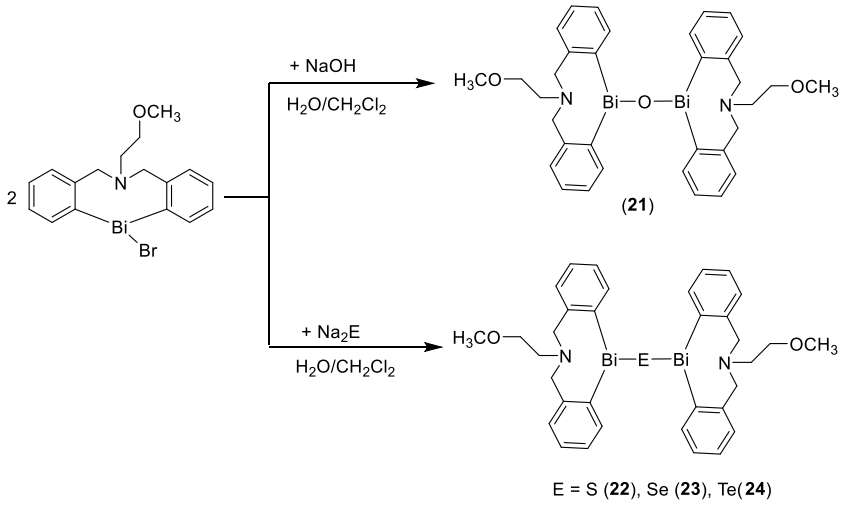

Scheme 6

In **Figure 18** are represented the ^{1}H NMR spectra of the dinuclear compound and the diorganobismuth(III) bromide. The ^{1}H NMR spectra suggest that in solution the nitrogen atom is coordinated to bismuth, and thus the H_7 protons in the methylene group become non-equivalent and appear in the form of an AB system. In comparison with the starting material, the resonances of compounds **21**-**24** are shifted.

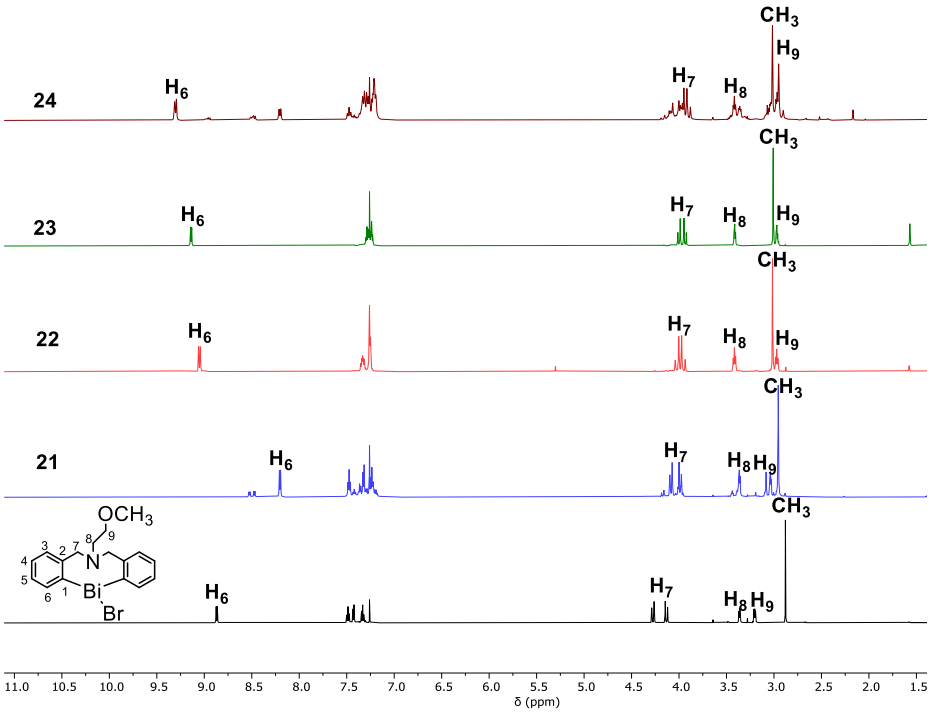

Figure 18. ^{1}H NMR spectra ($CDCl_3$, 400.13 MHz) of the compound $[CH_3OCH_2CH_2N(CH_2C_6H_4)_2Bi]_2O$ (**21**), $[CH_3OCH_2CH_2N(CH_2C_6H_4)_2Bi]_2S$ (**22**), $[CH_3OCH_2CH_2N(CH_2C_6H_4)_2Bi]_2Se$ (**23**), $[CH_3OCH_2CH_2N(CH_2C_6H_4)_2Bi]_2Te$ (**24**) and $[CH_3OCH_2CH_2N(CH_2C_6H_4)_2]BiBr$.

In case of compound **23**, during the growth of single crystals was observed the formation of a dinuclear species with the fragment BiOSe(O)OBi. The oxidation of the Se atom can be easily observed in the $^{77}Se\{^{1}H\}$ NMR spectrum. The resonance determined by the selenium(II) atom, unoxidized and attached to Bi, appears at the value δ = -223.5 ppm, while the signal determined by selenium(IV) was observed at the value δ = 1331.4 ppm. The molecular structure was determined by single crystal X-ray diffraction, and it confirms the oxidation of the selenium(II) to Se(IV) (**Figure 19**).

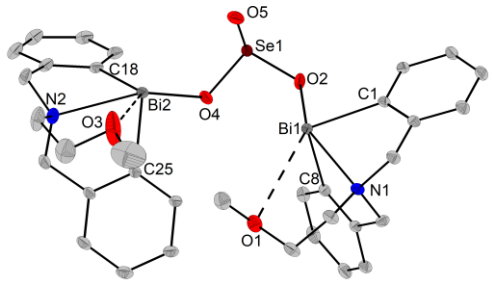

Figure 19. Thermal ellipsoids representation at 30% probability of the molecular structure of compound $[CH_3OCH_2CH_2N(CH_2C_6H_4)_2BiO]_2SeO$ (**23a**) Hydrogen atoms were omitted for clarity.

In the crystal of compound **23a** C–H···π intermolecular interactions were observed, with values in the range 2.894(1)-2.966(1) Å, as well as O···H intermolecular contacts, which contribute to the formation of a supramolecular structure (**Figure 20**).

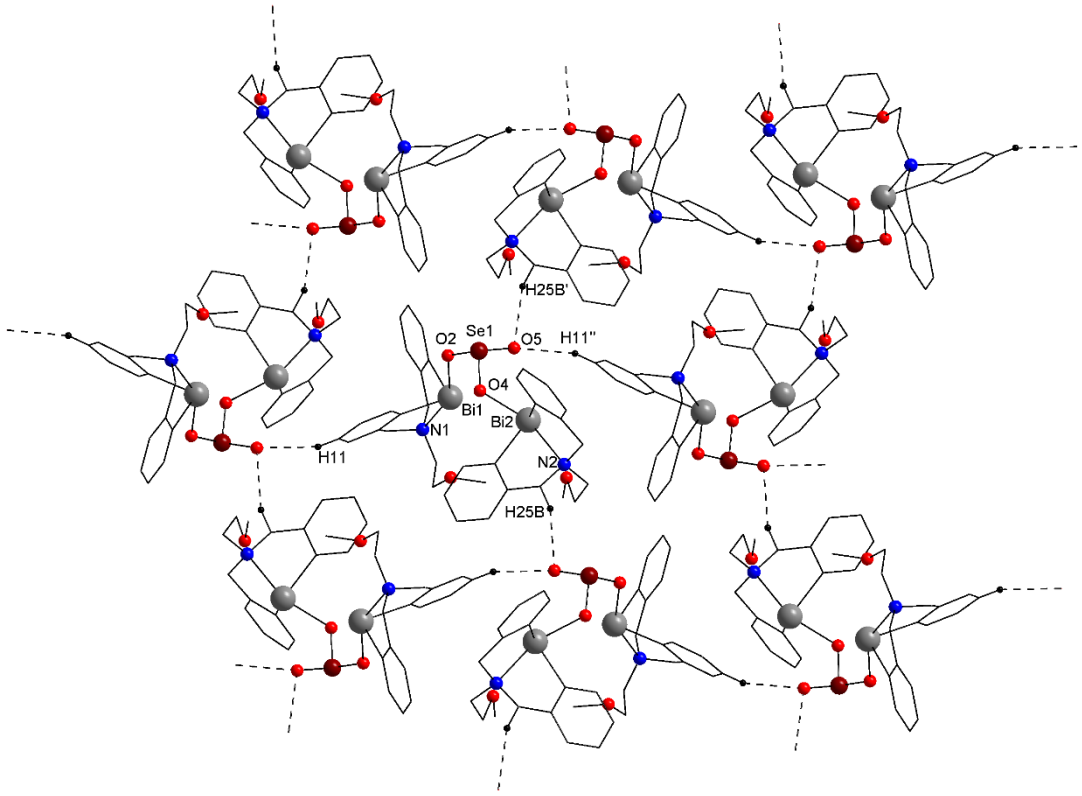

Figure 20. 2D supramolecular association in the crystal of compound $[CH_3OCH_2CH_2N(CH_2C_6H_4)_2BiO]_2SeO$ (**23a**) [symmetry operations: *-1/2+x, 3/2-y, 1/2+z* (')*; 3/2-x, 1/2+y, 3/2-z* (")]. Hydrogen atoms not involved in interactions were omitted for clarity.

III.2.2. Sb(III) complexes

III.2.2.1. Reactions of $[2\text{-}(Me_2NCH_2)C_6H_4SbO]_3$ with carboxylic acids

The reactivity of the organoantimony(III) oxide $[2\text{-}(Me_2NCH_2)C_6H_4SbO]_3$ was investigated towards acetic acid, monochloroacetic acid, dichloroacetic acid and trifluoroacetic acid, using 1 : 3 and a 1 : 6 molar ratio. The reactions were performed at room temperature, in dichloromethane, and led to the formation of six organoantimony(III) compounds, namely the compounds **25-30** (**Scheme 7**). Compounds **25**, **27** and **29** initially were obtained by reacting $[2\text{-}(Me_2NCH_2)C_6H_4SbO]_3$ and the appropriate acid in a 1 :3 molar ratio. The formation of compounds **25** and **27** was confirmed not only by NMR spectroscopy, but also by single X-ray diffraction.

The reactivity of the cyclic oxide $[2\text{-}(Me_2NCH_2)C_6H_4SbO]_3$ towards the trichloroacetic acid was different when compared with all the other investigated acids. With trichloroacetic acid, two compounds were isolated, namely compounds **26** and **30**.

Using different molar ratios, 1 : 3 and 1 : 6, two different compounds were isolated, which gave different resonances in the ^{1}H and $^{13}C\{^{1}H\}$ NMR spectra, and which had different melting points.

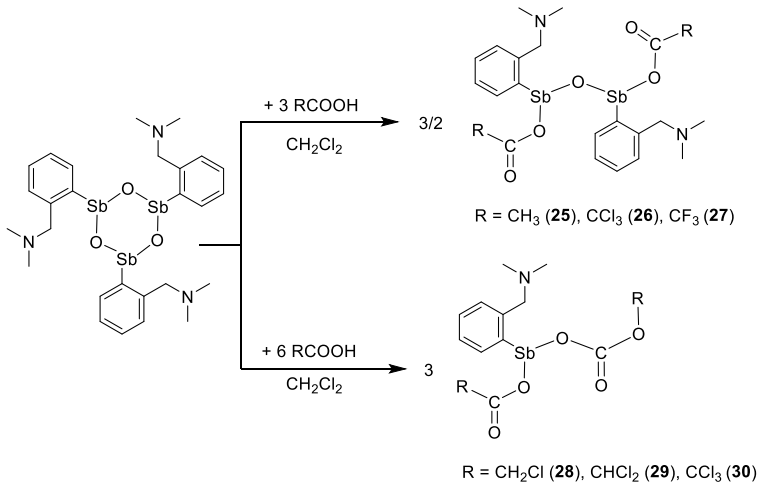

Scheme 7

In the aliphatic region of the ^{1}H NMR spectrum (**Figure 21**), the protons from the two methyl groups give a singlet resonance [δ 2.47 (**25**), 2.35 (**26**), 2.60 ppm (**27**)], which suggests that the two methyl groups in the pendant arm are equivalent. In compound **25** the protons from the methylene groups appear as a singlet (δ 3.92 ppm), instead in compounds **26** and **27** the protons from the methylene groups appear as an AB system, thus suggesting that in solution the nitrogen atom in the pendant arm coordinate to antimony, and the two protons from the methylene groups become non-equivalent in this way.

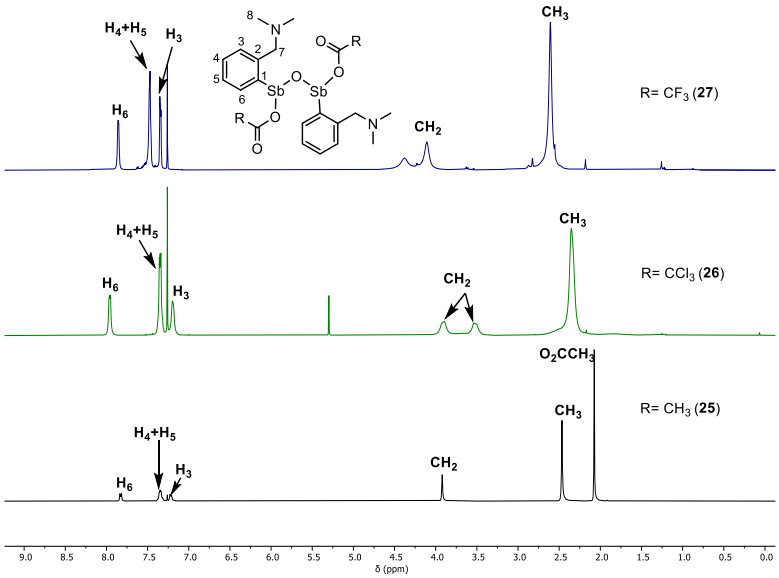

Figure 21. ^{1}H NMR spectra ($CDCl_3$) of compounds [2-(Me_2NCH_2)$C_6H_4SbOC(O)CH_3]_2O$ (**25**), [2-(Me_2NCH_2)$C_6H_4SbOC(O)CCl_3]_2O$ (**26**) and [2-(Me_2NCH_2)$C_6H_4SbOC(O)CF_3]_2O$ (**27**).

In the APCI+ mass spectra of compounds **25** and **27** (**Figure 22**) the peaks which correspond to the molecular ion were not observed, but peaks corresponding to the cation was observed $[M\text{-}CH_3C(O)O]^+$ (m/z 587.00944, the theoretical value being 587.00965) and $[M\text{-}CF_3C(O)O]^+$ (m/z 640.98057, the theoretical value being 640.98139). The base peak for both compounds corresponds to the fragment $[RSb(O)CH_3]^+$, having the experimental m/z value 256.00808 for the compound **25** and 256.00789 for the compound **27**, and the theoretical value being 256.00807. Another fragment identified for the compound **25** was $[RSbOC(O)CH_3]^+$ (experimental m/z 314.01354, and theoretical m/z value 314.01355), while for the compound **27** $[RSbOC(O)CF_3]^+$, with an experimental m/z value 367.98494 and a theoretically m/z value 367.98528.

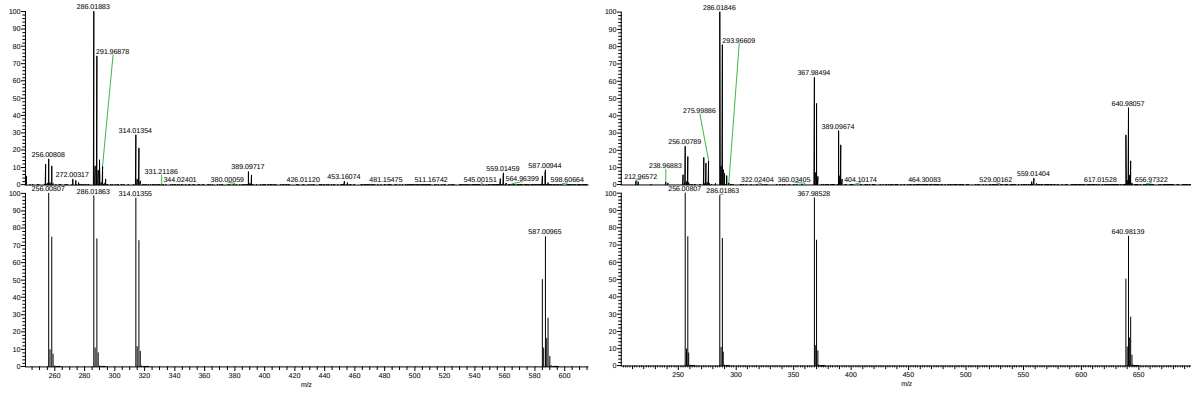

(a) (b)

Figure 22. Mass spectra for the compound $[2\text{-}(Me_2NCH_2)C_6H_4SbOC(O)CH_3]_2O$ (**25**) (a) and $[2\text{-}(Me_2NCH_2)C_6H_4SbOC(O)CF_3]_2O$ (**27**) (b) experimental (up) and calculated (down).

The molecular structures (**Figure 23**) of compounds **25**, **26** and **27** were determined by single crystal X-ray diffraction. In the three compounds it is observed that the acetate, trichloroacetate and trifluoroacetate fragments, respectively, coordinate anizobidentate to the two antimony atoms.

The coordination geometry around the antimony atoms in all three molecular structures is ψ-octahedral if both O–Sb interactions with the anionic ligands and the lone pair of electrons at antimony are considered. Both antimony atoms in compounds **25**, **26** and **27** are chiral centers. The compounds show also planar chirality, which results from the non-planarity of the pentaatomic heterocycles formed by the intramolecular coordination of nitrogen to antimony. In this way the crystals of the three compounds contain a racemic mixture of isomers.

In the crystal of the compound **25**, intermolecular C–H···π interactions and O···H contacts led to the formation of a 1D chain.

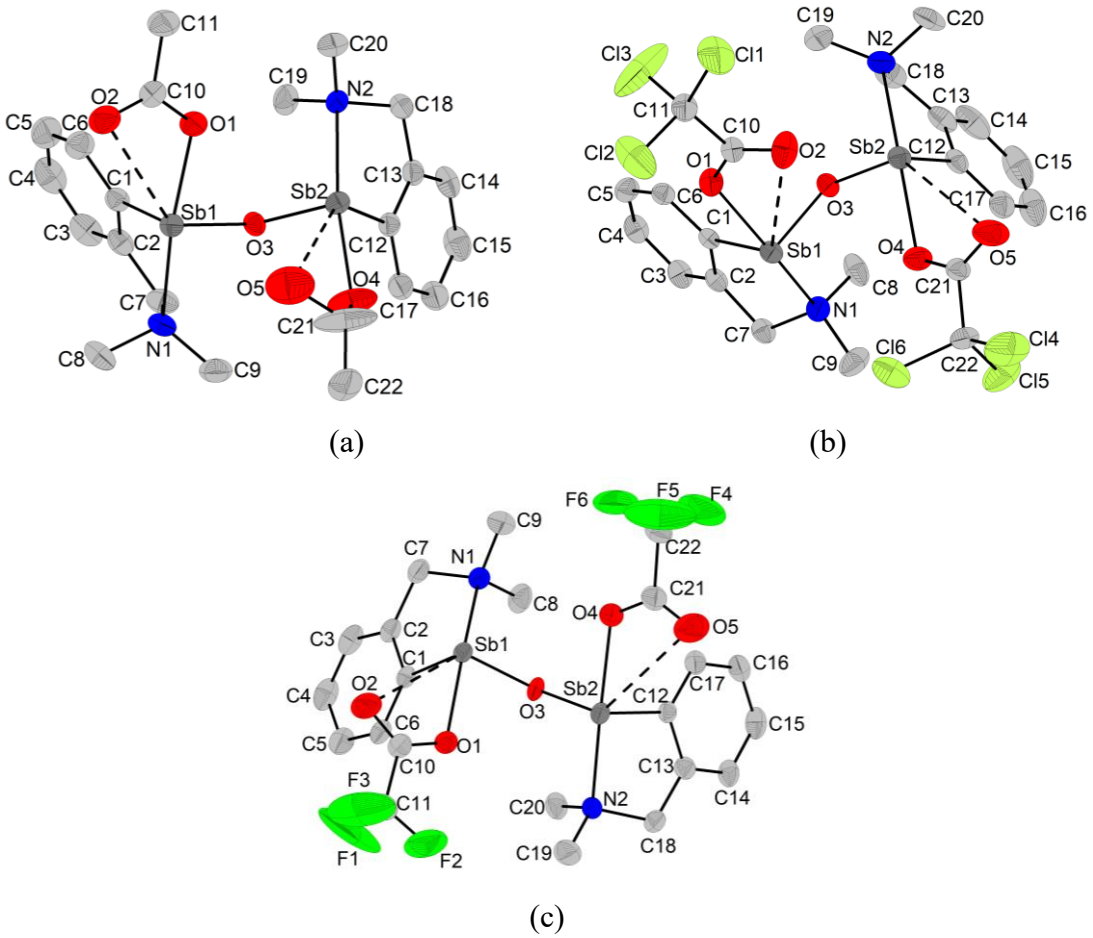

Figure 23. Thermal ellipsoids representations at 30% probability of the molecular of the compounds $[2\text{-}(Me_2NCH_2)C_6H_4SbOC(O)CH_3]_2O$ (**25**) (a), $[2\text{-}(Me_2NCH_2)C_6H_4SbOC(O)CCl_3]_2O$ (**26**) (b) and $[2\text{-}(Me_2NCH_2)C_6H_4SbOC(O)CF_3]_2O$ (**27**) (c). Hydrogen atoms were omitted for clarity.

In the aliphatic region of the $^{13}C\{^1H\}$ NMR spectra of compounds **28**, **29** and **30** signals characteristic to the carbon atoms from the acetate, CH_2Cl, and $CHCl_2$ groups, respectively, are observed, as well as signals characteristic to the carbon atoms in the fragment 2-(*N,N*-dimethylaminomethyl). In the aromatic region seven resonances were observed, corresponding to the aromatic carbons from the 2-(*N,N*-dimethylaminomethyl)phenyl moiety and one resonance corresponding to the carbon in the carboxyl group (**Figure 24**).

.

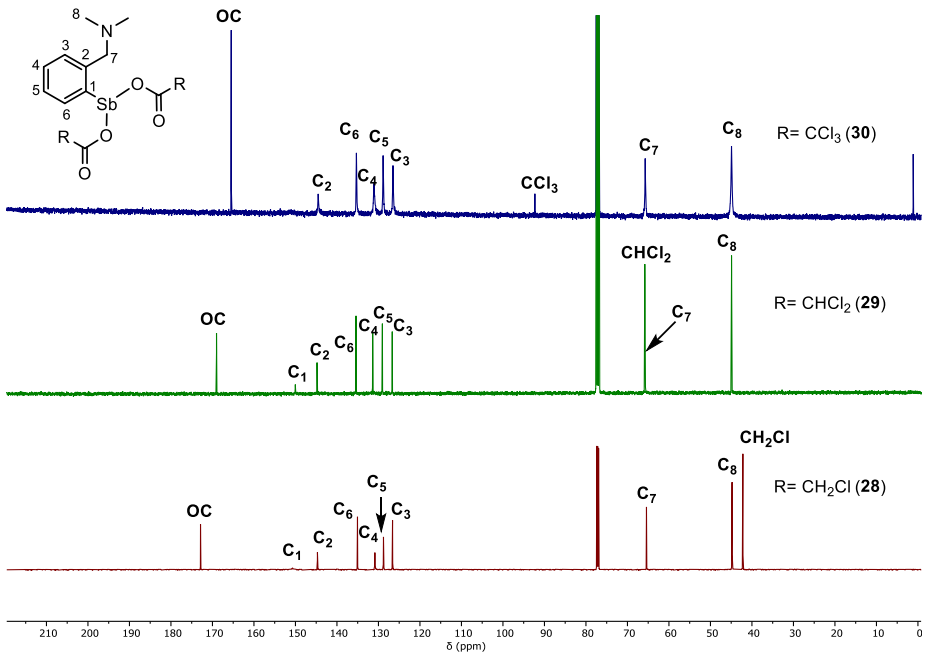

Figure 24. $^{13}C\{^{1}H\}$ NMR spectra ($CDCl_3$) of the compound 2-$(Me_2NCH_2)C_6H_4Sb[OC(O)CH_2Cl]_2$ (**28**), 2-$(Me_2NCH_2)C_6H_4Sb[OC(O)CHCl_2]_2$ (**29**) and 2-$(Me_2NCH_2)C_6H_4Sb[OC(O)CCl_3]_2$ (**30**).

The APCI+ mass spectra for compounds **28** and **29** were determined in methanol. The molecular ion was not observed for these compounds, and the base peak for compound **28** corresponds to the cation $[RSbCl]^+$ at the m/z value 289.9694, while for compound **29** the base peak corresponds to the fragment $[RSbCl+H]^+$ at the m/z value 291.96884.

Single crystals were obtained only for compound **28**. The molecular structure for **28** was determined by single crystal X-ray diffraction, and it is represented in **Figure 25**. It was observed that the 2-$(Me_2NCH_2)C_6H_4$ group behaves as a *C*,*N*-chelating ligand towards antimony, while the monochloroacetato ligands act as bidentate moieties [Sb–O 2.985(6)/2.987(6) Å, Σ_{rvdW}(Sb,O) = 3.60 Å[67]], thus resulting in a distorted octahedral geometry around the metal.

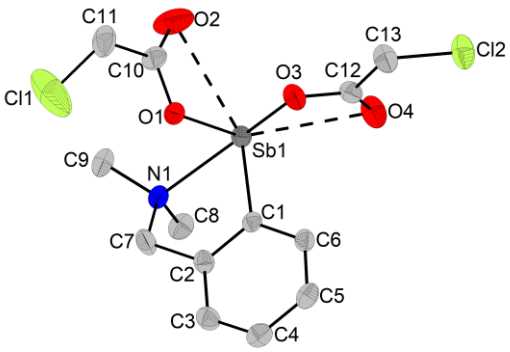

Figure 25. Thermal ellipsoids representation at 30% probability of the molecular structure of the compound 2-$(Me_2NCH_2)C_6H_4Sb[OC(O)CH_2Cl]_2$ (**28**). Hydrogen atoms were omitted for clarity.

Due to the N→Sb intramolecular coordination, compound **28**, as well as compounds **25-27**, present planar chirality. The antimony atom becomes chiral due to the disposal of the donor atoms around the metal. As a result, the crystal of compound **28** contains a racemic mixture of isomers, namely A_{Sb},pS_N (**Figure 25**) and C_{Sb},pR_N, where *A* and *C* refer to the chirality of antimony, and *pR* and *pS* to the planar chirality.

In the crystal O···H intermolecular interactions were observed: O2···H9B 2.490(6) Å and O4···H11B 2,462(4) Å (**Figure 26**) are observed, which led to the formation of a 2D supramolecular structure.

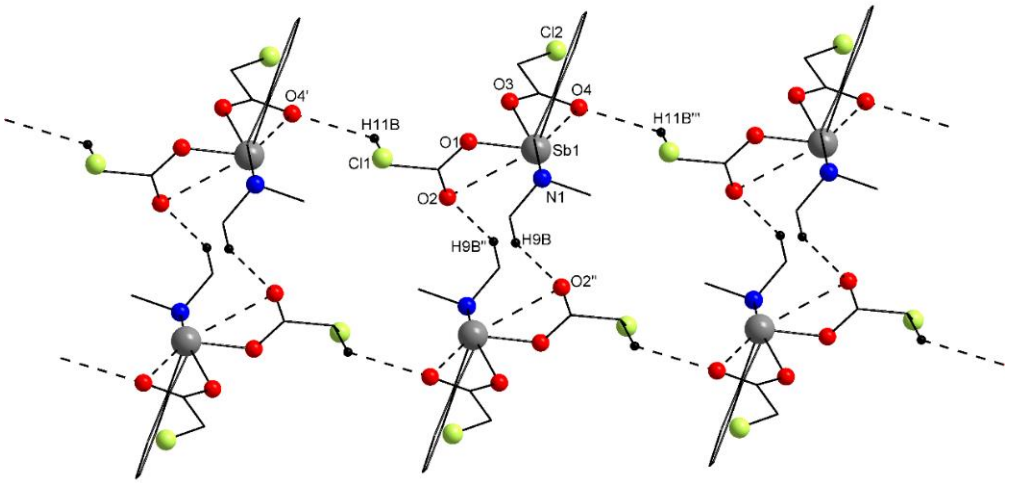

Figure 26. 2D network in the compound 2-(Me_2NCH_2)C_6H_4Sb(OC(O)CH_2Cl)$_2$ (**28**) [symmetry operation: 1+x, y, z ('); 1-x, -y, -z (''); -1+x, y, z (''')]. Hydrogen atoms not involved in interactions were omitted for clarity.

III.2.2.2. Reactions of [2-(Me_2NCH_2)C_6H_4SbO]$_3$ with trifluoromethanesulfonic acid and whit pentafluorophenol

The cyclic trimer [2-(Me_2NCH_2)C_6H_4SbO]$_3$ was reacted with pentafluorophenol, using either a 1 : 3 or a 1 : 6 molar ratio, and compounds **31** and **32** were isolated (**Scheme 8**).

The reactivity of the trimer [2-(Me_2NCH_2)C_6H_4SbO]$_3$ towards trifluoromethanesulfonic acid was similar to that observed for acetic acid. Although a 1 : 6 molar ratio, or even a higher excess of acid was used, the resulting compound was complex **33**.

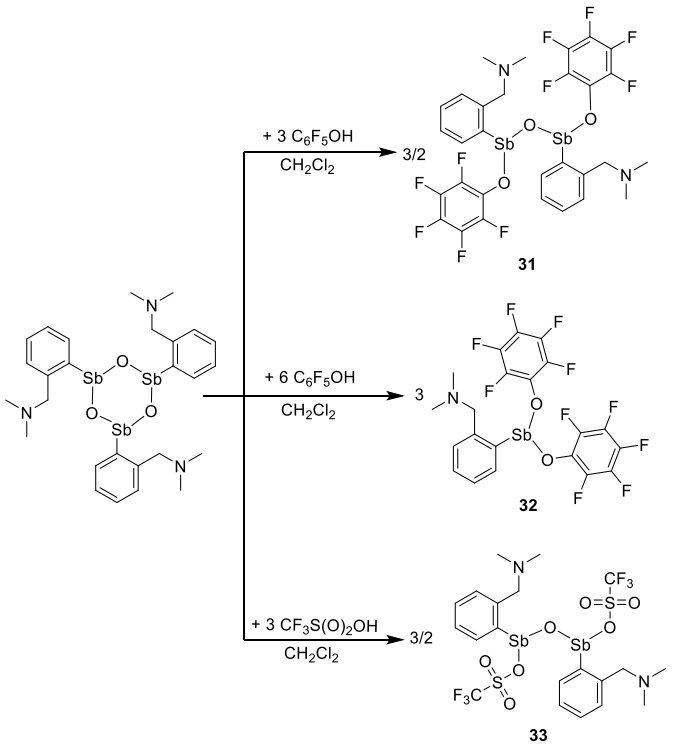

Scheme 8

The ^{1}H NMR spectra for compounds **31** and **32** are depicted in **Figure 27**.

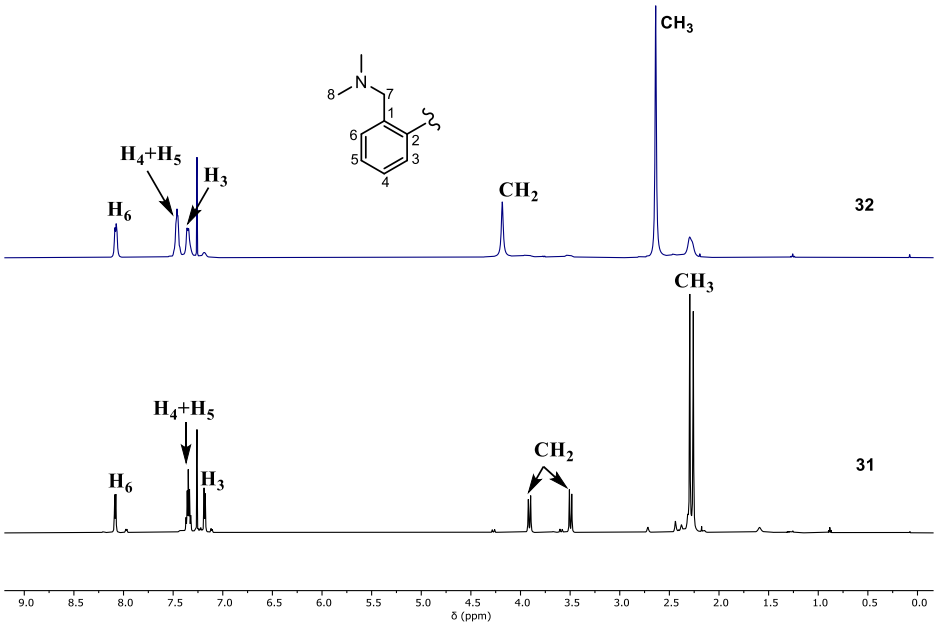

Figure 27. ^{1}H NMR spectra ($CDCl_3$) of compounds $[2\text{-}(Me_2NCH_2)C_6H_4SbOC_6F_5]_2O$ (**31**) and $2\text{-}(Me_2NCH_2)C_6H_4Sb(OC_6F_5)_2$ (**32**).

For the compounds **31** and **32** the ^{19}F{^{1}H} NMR spectra were recovered. For both compounds three sets of signals were observed.

For compound **32** the molecular structure (**Figure 28**) was determined by single crystal X-ray diffraction and the coordination of the nitrogen atom to antimony was observed. The coordination geometry around the antimony atom is trigonal ψ-bipyramidal, with an oxygen atom of a pentafluorophenoxo fragment and the nitrogen atom from the pendant arm in apices.

In the crystal were observed intermolecular interactions, namely Sb···F [Sb1···F2 3.841(5) Å, Sb1···F3 3.701(6) Å and Sb1···F7 3.846(7) Å, cf. Σ_{rvdW}(Sb, F) = 3.93 Å[67]], F···H [F6···H9C 2.547(6) Å, F8···H9A 2.528(6) Å, cf. Σ_{rvdW}(F, H) = 2.66 Å[67]] and $\pi\cdots\pi$ [3.686(5) Å, established between C10-C15 pentafluorophenoxo groups, which led to a 3D supramolecular network.

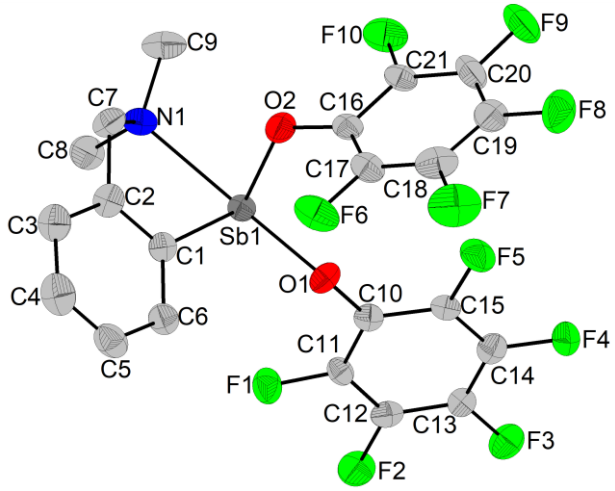

Figure 28. Thermal ellipsoids representation at 30% probability of the molecular structures of the compound 2-(Me_2NCH_2)$C_6H_4Sb(OC_6F_5)_2$ **(32)**. Hydrogen atoms were omitted for clarity.

III.2.2.3. Reactions of [2-(Me_2NCH_2)$C_6H_4SbO]_3$ with tetraphenyldichalcogenoimidodiphosphinic acids

Reactions were performed between the cyclic compound [2-(Me_2NCH_2)$C_6H_4SbO]_3$ and tetraphenyldichalcogenoimidodiphosphinic acids, namely [($Ph_2PO)_2N$]H, (Ph_2PO)(Ph_2PS)NH and ($Ph_2PS)_2$NH, which led to the formation of compounds **34**, **35** and **36**. The reactions were performed in dichloromethane, at room temperature, using a 1 : 3 molar ratio (**Scheme 9**).

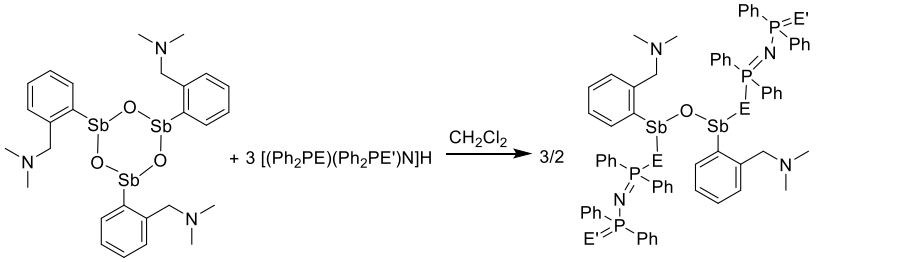

Scheme 9

The formation of compounds **34**, **35** and **36** was monitored by NMR (^{1}H, ^{13}C{^{1}H}, ^{31}P{^{1}H}) spectroscopy. The ^{1}H and ^{31}P{^{1}H} NMR spectra were recorded both at room temperature and at variable temperature (**Figure 29** and **Figure 30**).

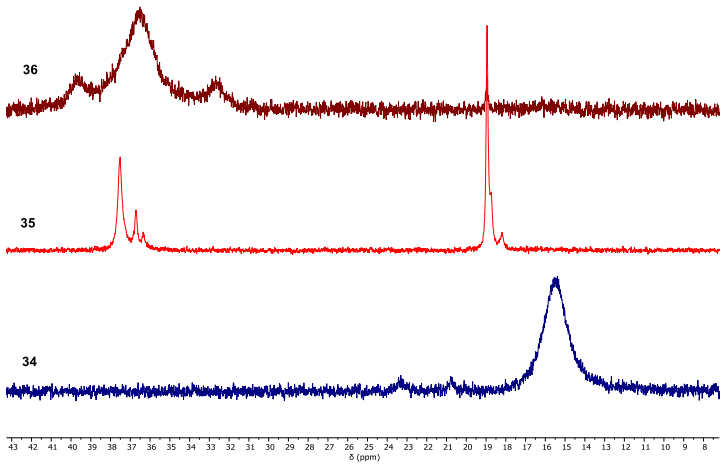

Figure 29. ^{31}P{^{1}H} NMR spectra ($CDCl_3$, 161.97 MHz) of [2-(Me_2NCH_2)C_6H_4Sb{$OPPh_2NP(O)Ph_2$}]$_2$O (**34**), [2-(Me_2NCH_2)C_6H_4Sb{$OPPh_2NP(S)Ph_2$}]$_2$O (**35**) and [2-(Me_2NCH_2)C_6H_4Sb{$SPPh_2NP(S)Ph_2$}]$_2$O (**36**).

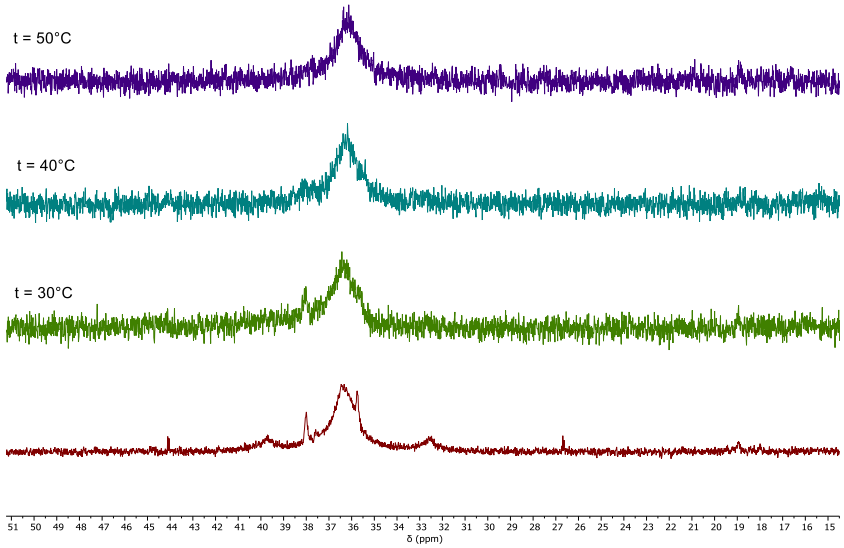

Figure 30. ^{31}P{^{1}H} NMR spectra ($CDCl_3$, 161.97 MHz) of the compound [2-(Me_2NCH_2)C_6H_4Sb{$SPPh_2NP(S)Ph_2$}]$_2$O (**36**) at variable temperature.

The NMR spectra suggest the existence of a mixture of species in solution, determined rather by a fluxional behaviour than by decomposition.

Single crystals of the compound **35** were obtained from a mixture of solvents, dichloromethane/hexane (1 : 4, v/v). The molecular structure (**Figure 31**) showed that the nitrogen atoms from the pendant arms coordinate intramolecularly to the two antimony atoms.

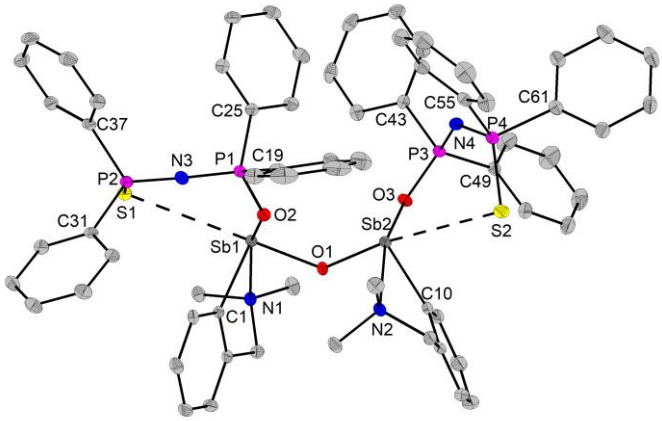

Figure 31. Thermal ellipsoids representation at 30% probability of the molecular structure of [2-(Me_2NCH_2)C_6H_4SbOPPh_2NP(S)Ph_2]$_2$O (**35**). Hydrogen atoms were omitted for clarity.

It was also observed that the dichalcogenoimidodiphosphinato ligand [(OPPh_2)(SPPh_2)N]$^-$, is coordinated in a bidentate, *O,S*-chelating fashion to the two antimony atoms. The coordination number at antimony is 5, and the compound **35** can be described as a hypervalent *12–Sb–5* species. The coordination geometry around both antimony atoms can be described as a square pyramid ($\tau_{5,\,Sb1}$ = 0.12, $\tau_{5,\,Sb2}$ = 0.13),[73,74] with the *ipso* carbon atoms in apical positions. Both antimony atoms are chiral centers, with four different substituents around each of them, namely one nitrogen atom from the pendant arm, two oxygen atoms and one sulphur atom. The 2-(Me_2NCH_2)C_6H_4Sb fragments show planar chirality and, as a result, the crystal of this compound contains $C_{Sb1}R_{N1}C_{Sb2}R_{N2}$ and $A_{Sb1}S_{N1}A_{Sb2}S_{N2}$ isomers.

The molecular structure of compound **36** (**Figure 32**) was determined also by single crystal X-ray diffraction. The crystal of compound **36** contains a racemic mixture of $A_{Sb1}R_{N1}A_{Sb2}S_{N2}$ and $C_{Sb1}R_{N1}C_{Sb2}R_{N2}$ isomers.

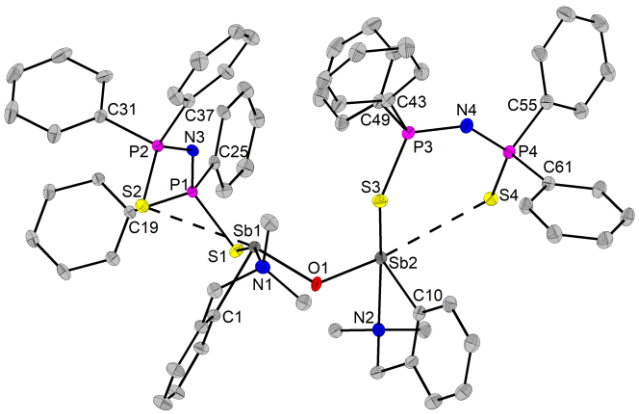

Figure 32. Thermal ellipsoids representation at 30% probability of the molecular structure of [2-(Me_2NCH_2)C_6H_4SbSPPh_2NP(S)Ph_2]$_2$O (**36**). Hydrogen atoms were omitted for clarity.

III.3. Conclusions

Four dinuclear diorganobismuth(III) compounds which contain a *C,N,C*-Bi fragment, with a butterfly-like skeleton, namely $CH_3OCH_2CH_2N(CH_2C_6H_4)_2Bi]_2O$ (**21**), $[CH_3OCH_2CH_2N(CH_2C_6H_4)_2Bi]_2S$ (**22**), $[CH_3OCH_2CH_2N(CH_2C_6H_4)_2Bi]_2Se$ (**23**) and $[CH_3OCH_2CH_2N(CH_2C_6H_4)_2Bi]_2Te$ (**24**) were synthetised. In all these compounds it was observed that in solution the nitrogen atom coordinates to the bismuth atom.

The dinuclear compound $[CH_3OCH_2CH_2N(CH_2C_6H_4)_2Bi]_2Te$ (**24**) was obtained in mixture with a species containing the fragment $R_2Te{=}O$, and it was observed that in time the two compounds are not stable and they underwent a decomposition process.

The compound $[CH_3OCH_2CH_2N(CH_2C_6H_4)_2Bi]_2Se$ (**23**) was oxidized in time as well, and the compound $[CH_3OCH_2CH_2N(CH_2C_6H_4)_2BiO]_2SeO$ (**23a**) was formed. The molecular structure determined by single crystal X-ray diffraction confirmed the above formula of **23a**. The compound is a *12–Bi–5* hypervalent species. In the crystal was observed the formation of a 2D supramolecular network by O···H intermolecular interactions.

The base peaks in the APCI+ mass spectra of compounds **22** and **23** correspond to the fragment $[CH_3OCH_2CH_2N(CH_2C_6H_4)_2Bi]^+$.

The reaction between the trimeric cycle $[2\text{-}(Me_2NCH_2)C_6H_4SbO]_3$ with different carboxylic acids, namely acetic acid, monochloroacetic acid, dichloroacetic acid, trichloroacetic acid and trifluoroacetic acid, in a 1 : 3 or a 1 : 6 molar ratio, led to the formation of six new compounds: $[2\text{-}(Me_2NCH_2)C_6H_4SbOC(O)CH_3]_2O$ (**25**), $[2\text{-}(Me_2NCH_2)C_6H_4SbOC(O)CCl_3]_2O$ (**26**), $[2\text{-}(Me_2NCH_2)C_6H_4SbOC(O)CF_3]_2O$ (**27**), $2\text{-}(Me_2NCH_2)C_6H_4Sb[OC(O)CH_2Cl]_2$ (**28**), $2\text{-}(Me_2NCH_2)C_6H_4Sb[OC(O)CHCl_2]_2$ (**29**), $2\text{-}(Me_2NCH_2)C_6H_4Sb[OC(O)CCl_3]_2$ (**30**).

The molecular structures of compounds **25**-**28** were determined by single crystal X-ray diffraction. In all these structures was observed the intramolecular coordination of the nitrogen atom in the pendant arm to antimony. In the crystals of these compounds were observed intermolecular interactions of type C–H···π, O···H and/or Cl···H, that led to the formation of supramolecular structures.

The reactions of the cyclic trimer $[2\text{-}(Me_2NCH_2)C_6H_4SbO]_3$ with pentafluorophenol and, respectively, with trifluoromethanesulfonic acid, using a 1 : 3 or a 1 : 6 molar ratio, led to the formation of three new compounds: $[2\text{-}(Me_2NCH_2)C_6H_4SbOC_6F_5]_2O$ (**31**), $2\text{-}(Me_2NCH_2)C_6H_4Sb(OC_6F_5)_2$ (**32**) and $[2\text{-}(Me_2NCH_2)C_6H_4SbO_2S(O)CF_3]_2O$ (**33**). For the compound $2\text{-}(Me_2NCH_2)C_6H_4Sb(OC_6F_5)_2$ (**32**) the molecular structure was determined by

single crystal X-ray diffraction and it was observed that the two pentafluorophenoxi groups are not equivalent, and the Sb···F and F···H interactions led to the formation of a 3D supramolecular network.

The reactions between the cyclic compound $[2\text{-}(Me_2NCH_2)C_6H_4SbO]_3$ and tetraphenyldichalcogenoimidodiphosphinic acids $[(Ph_2PO)_2N]H$, $(Ph_2PO)(Ph_2PS)NH$ and $(Ph_2PS)_2NH$, using a 1 : 3 molar ration, led to the formation of compounds $[2\text{-}(Me_2NCH_2)C_6H_4Sb\{OPPh_2NP(O)Ph_2\}]_2O$ (**34**), $[2\text{-}(Me_2NCH_2)C_6H_4Sb\{OPPh_2NP(S)Ph_2\}]_2O$ (**35**) and $[2\text{-}(Me_2NCH_2)C_6H_4Sb\{SPPh_2NP(S)Ph_2\}]_2O$ (**36**).

For compounds $[2\text{-}(Me_2NCH_2)C_6H_4Sb\{OPPh_2NP(S)Ph_2\}]_2O$ (**35**) and $[2\text{-}(Me_2NCH_2)C_6H_4Sb\{SPPh_2NP(S)Ph_2\}]_2O$ (**36**) the molecular structure was determined by single crystal X-ray diffraction. Both compound $[2\text{-}(Me_2NCH_2)C_6H_4Sb\{OPPh_2NP(S)Ph_2\}]_2O$ (**35**) and $[2\text{-}(Me_2NCH_2)C_6H_4Sb\{SPPh_2NP(S)Ph_2\}]_2O$ (**36**) are *12–Sb–5* hypervalent species.

For compounds **34-36** are necessary supplementary investigations to elucidate their behaviour in solution.

V. BIBLIOGRAPHY

1 J. R. Gispert, *Coordination Chemistry*, Wiley-VCH, New York, 2008.

2 U. B. Kim, D. J. Hyun, H. J. Jeon, K. Rathwell and S. Lee, *Chem. Rev.*, 2020, **120**, 13382–13433.

3 B. K. Keppler (Ed.), *Metal Complexes in Cancer Chemotherapy*, Wiley-VCH, New York, 1993.

4 A. Burini, R. Bravi, J. P. Fackler, R. Galassi, T. A. Grant, M. A. Omary, B. R. Pietroni and R. J. Staples, *Inorg. Chem.*, 2000, **39**, 3158–3165.

5 M. Chiarucci and M. Bandini, *Beilstein J. Org. Chem.*, 2013, **9**, 2586–2614.

6 C. Silvestru, H. J. Breunig and H. Althaus, *Chem. Rev.*, 1999, **99**, 3277–3327.

7 C. I. Raţ, C. Silvestru and H. J. Breunig, *Coord. Chem. Rev.*, 2013, **257**, 818–879.

8 A. G. Davies, M. Gielen, K. H. Pannell and E. R. T. Tiekink (Eds.), *Tin Chemistry: Fundamentals, Frontiers, and Applications, John Wiley & Sons*, Ltd, Chichester, 2008.

9 K. -ya Akiba (Ed), *Chemistry of Hypervalent Compounds*, Wiley-VCH, New York, 1999.

10 J. J. Li and W. M. Zhu, *Acta Crystallogr.*, 2012, **E68**, m845.

11 P. Pyykkö, *Chem. Rev.*, 1997, **97**, 597–636.

12 C. P. Rây, N. Adhikari and H. Rây, *J. Indian Chem. Soc.*, 1931, **8**, 689.

13 J. K. Wrobel, R. Power and M. Toborek, *IUBMB Life*, 2016, **68**, 97–105.

14 J. H. Perras, S. M. J. Mezibroski, M. A. Wiebe and J. S. Ritch, *Dalton Trans.*, 2018, **47**, 1471–1478.

15 J. B. T. Rocha, B. C. Piccoli and C. S. Oliveira, *Arkivoc*, 2017, **ii**, 457–491.

16 G. F. Combs and W. P. Gray, *Pharmacol. Ther.*, 1998, **79**, 179–192.

17 A. P. Fernandes and V. Gandin, *Biochim. Biophys. Acta, Gen. Subj.*, 2015, **1850**, 1642–1660.

18 I. Di Leo, F. Messina, V. Nascimento, F. G. Nacca, D. Pietrella, E. J. Lenardão, G. Perin and L. Sancineto, *Mini-Rev. Org. Chem.*, 2019, **16**, 589–601.

19 C. Santi (Ed.), *Organoselenium Chemistry. Between Synthesis and Biochemistry*, Bentham Books, 2014.

20 A. Müller, E. Cadenas, P. Graf and H. Sies, *Biochem. Pharmacol.*, 1984, **33**, 3235–3239.

21 P. L. Caradoc-Daviesa, L. R. Hanto and W. Henderson, *J. Chem. Soc. Dalton Trans.*, 2001, 2749–2755.

22 S. Mishra, D. Du, E. Jeanneau, F. Dappozze, C. Guillard, J. Zhang and S. Daniele, *Chem. Asian J.*, 2016, **11**, 1658–1663.

23 K. N. Sharma, A. K. Sharma, H. Joshi and A. K. Singh, *ChemistrySelect*, 2016, **1**, 3573–3579.

24 C. Wei, Z. Li and C. J. Li, *Org. Lett.*, 2003, **5**, 4473–4475.

25 P. T. Anastas and J. C. Warner, *Theory and Practice*, Oxford University Prees, Oxford, 1998.

26 A. A. Lysova, R. D. Marchenko, D. G. Samsonenko, A. S. Potapov and V. P. Fedin, *Russ. Chem. Bull.*, 2020, **69**, 1122–1129.

27 R. D. Marchenko, A. A. Lysova, D. G. Samsonenko, D. N. Dybtsev and A. S. Potapov, *Polyhedron*, 2020, **177**, 114330.

28 R. Cargnelutti, A. Hagenbach, U. Abram, R. A. Burrow and E. S. Lang, *Polyhedron*, 2015, **96**, 33–37.

29 M. J. Poropudas, L. Vigo, R. Oilunkaniemi and R. S. Laitinen, *Dalton Trans.*, 2013, **42**, 16868–16877.

30 M. Risto, T. T. Takaluoma, T. Bajorek, R. Oilunkaniemi, R. S. Laitinen and T. Chiver, *Inorg. Chem.*, 2009, **48**, 6271–6279.

31 M. Munakata, L. P. Wu, T. Kuroda-Sowa, M. Maekawa, Y. Suenaga and S. Nakagawa, *J. Chem. Soc., Dalton Trans.*, 1996, 1525–1530.

32 M. O. Awaleh, A. Badia and F. Brisse, *Inorg. Chem.*, 2005, **44**, 7833–7845.

33 C. R. van den Brom, M. Wagner, V. Enkelmann, K. Landfester and C. K. Weiss, *Langmuir*, 2010, **26**, 15794–15801.

34 J. Fielden, D. Long, A. M. Z. Slawin, P. Kogerles and L. Cronin, *Inorg. Chem.*, 2007, **46**, 9090–9097.

35 W. Levason, M. Nirwan, R. Ratnani, G. Reid, N. Tsoureas and M. Webster, *Dalton Trans.*, 2007, 439–448.

36 S. Ž. Đurić, M. Mojicevic, S. Vojnovic, H. Wadepohl, T. P. Andrejević, N. L. Stevanović, J. Nikodinovic-Runic, M. I. Djuran and B. Glišić, *Inorg. Chim. Acta*, 2020, **502**, 119357.

37 M. Q. Granato, T. P. Mello, R. S. Nascimento, M. D. Pereira, T. L. S. A. Rosa, M. C. V. Pessolani, M. McCann, M. Devereux, M. H. Branquinha, A. L. S. Santos and L. F. Kneipp, *Front. Microbiol.*, 2021, **12**, 1–12.

38 A. C. M. Galdino, L. Viganor, M. M. Pereira, M. Devereux, M. McCann, M. H. Branquinha, Z. Molphy, S. O'Carroll, C. Bain, G. Menounou, A. Kellett and A. L. S. dos Santos, *JBIC, J. Biol. Inorg. Chem.*, 2022, **27**, 201–213.

39 J. C. Mather, J. A. Wyllie, A. Hamilton, T. P. Soares da Costa and P. J. Barnard, *Dalton Trans.*, 2022, **51**, 12056–12070.

40 R. Rowan, T. Tallon, A. M. Sheahan, R. Curran, M. McCann, K. Kavanagh, M. Devereux and V. McKee, *Polyhedron*, 2006, **25**, 1771–1778.

41 M. E. K. Stathopoulou, C. N. Banti, N. Kourkoumelis, A. G. Hatzidimitriou, A. G. Kalampounias and S. K. Hadjikakou, *J. Inorg. Biochem.*, 2018, **181**, 41–55.

42 R. Cargnelutti, F. D. da Silva, U. Abram and E. S. Lang, *New J. Chem.*, 2015, **39**, 7948–7953.

43 G. Kedarnath and V. K. Jain, *Coord. Chem. Rev.*, 2013, **257**, 1409–1435.

44 R. Cargnelutti, E. S. Lang, P. Piquini and U. Abram, *Inorg. Chem. Commun.*, 2014, **45**, 48–50.

45 M. O. Awaleh, A. Badia and F. Brisse, *Cryst. Growth Des.*, 2005, **5**, 1897–1906.

46 M. O. Awaleh, A. Badia, F. Brisse and X. H. Bu, *Inorg. Chem.*, 2006, **45**, 1560–1574.

47 Y. Zheng, J. R. Li, M. Du, R. Q. Zou and X. H. Bu, *Cryst. Growth Des.*, 2005, **5**, 215–222.

48 X. H. Bu, W. Chen, W. F. Hou, M. Du, R. H. Zhang and F. Brisse, *Inorg. Chem.*, 2002, **41**, 3477–3482.

49 X. H. Bu, Y. B. Xie, J. R. Li and R. H. Zhang, *Inorg. Chem.*, 2003, **42**, 7422–7430.

50 C. L. Chen, Z. Q. Yu, Q. Zhang, M. Pan, J. Y. Zhang, C. Y. Zhao and C. Y. Su, *Cryst. Growth Des.*, 2008, **8**, 897–905.

51 C. L. Chen, C. Y. Su, Y. P. Cai, H. X. Zhang, A. W. Xu, B. S. Kang and H. C. zur Loye, 2003, **42**, 3738–3750.

52 J. R. Li, R. H. Zhang and X. H. Bu, *Cryst. Growth Des.*, 2003, **3**, 829–835.

53 R. A. Popa, M. David, E. Licarete, M. Banciu and A. Silvestru, *New J. Chem.*, 2022, **46**, 23019–23029.

54 M. David, R. Mitea and A. Silvestru, *J. Mol. Struct.*, 2021, **1246**, 131243.

55 M. De Franco, M. Saab, M. Porchia, C. Marzano, S. P. Nolan, F. Nahra, K. van Hecke and V. Gandin, *Chem. - Eur. J.*, 2022, **28**, e202201898.

56 M. Saab, D. J. Nelson, N. V. Tzouras, T. A. C. A. Bayrakdar, S. P. Nolan, F. Nahra and K. van Hecke, *Dalton Trans.*, 2020, **49**, 12068–12081.

57 R. A. Butuza, D. Dumitraş, C. Bohan and A. Pop, *New J. Chem.*, 2023, **47**, 2202–2210.

58 T. N. Srivastava, J. D. Singh and S. Srivastava, *Indian J. Chem., Sect. A: Inorg. Phys. Theor. Anal.*, 1989, **28**, 422–424.

59 I. Brito, M. López-Rodríguez, D. Vargas and A. Cárdenas, *Acta Crystallogr. Sect. E Struct. Rep. Online*, 2005, **61**, m2626–m2628.

60 H. Zhang, L. Chen, H. Song and G. Zi, *Inorg. Chim. Acta*, 2011, **366**, 320–336.

61 L. M. Chiang, C. W. Yeh, Z. K. Chan, K. M. Wang, Y. C. Chou, J. D. Chen, J. C. Wang and J. Y. Lai, *Cryst. Growth Des.*, 2008, **8**, 470–477.

62 A. J. Blake, N. R. Champness, P. A. Cooke, J. E. B. Nicolson and C. Wilson, *J. Chem. Soc, Dalton Trans.*, 2000, 3811–3819.

63 Y. Hiruta, T. Watanabe, E. Nakamura, N. Iwasawa, H. Sato, K. Hamada, D. Citterio and K. Suzuki, *RSC Adv.*, 2014, **4**, 9791–9798.

64 J. C. DeMott, F. Basuli, U. J. Kilgore, B. M. Foxman, J. C. Huffman, O. V. Ozerov and D. J. Mindiola, *Inorg. Chem.*, 2007, 46, 6271–6276.

65 S. L. Benjamin, L. Karagiannidis, W. Levason, G. Reid and M. C. Rogers, *Organometallics*, 2011, **30**, 895–904.

66 D. L. Klayman and T. S. Griffin, *J. Am. Chem. Soc.*, 1973, **2**, 197–199.

67 S. Alvarez, *Dalton Trans.*, 2013, **42**, 8617–8636.

68 W. J. Geary, *Coord. Chem. Rev.*, 1971, **7**, 81–122.

69 I. Ali, W. A. Wani and K. Saleem, *Synth. React. Inorg., Met.-Org., Nano-Met. Chem.*, 2013, **43**, 1162–1170.

70 K. S. Eccles, C. J. Elcoate, S. E. Lawrence and A. R. Maguire, *Arkivoc*, 2010, **ix**, 216–228.

71 P. M. Dickson, M. A. D. McGowan, B. Yearwood, M. J. Heeg and J. P. Oliver, *J. Organomet. Chem.*, 1999, **588**, 42–50.

72 T. Otsubo, F. Ogura, H. Yamaguchi, H. Higuchi and S. Misumi, *Synth. Commun.*, 1980, **10**, 595–601.

73 A. W. Addison, N. T. Rao, J. Reedijk, J. Rijn van and G. C. Verschoor, *J. Chem. Soc., Dalton Trans.*, 1984, 1349–1356.

74 L. Yang, D. R. Powell and R. P. Houser, *Dalton Trans.*, 2007, 955–964.

75 S. S. Sadhu, S. Wang, R. K. Averineni, T. Seefeldt, Y. Yang and X. Guan, *Melanoma Res.*, 2016, **26**, 572–579.

76 M. Postel and E. Duñach, *Coord. Chem. Rev.*, 1996, **155**, 127–144.

77 N. M. Leonard, L. C. Wieland and R. S. Mohan, *Tetrahedron*, 2002, **58**, 8373–8397.

78 A. Picot, S. Répichet, C. Le Roux, J. Dubac and N. Roques, *J. Fluorine Chem.*, 2002, **116**, 129–134.

79 H. Gaspard-Iloughmane and C. Le Roux, *Eur. J. Org. Chem.*, 2004, 2517–2532.

80 H. Suzuki and M. Yoshihiro (Eds.), *Organobismuth chemistry*, Elsevier., Amsterdam, 2001.

81 P. Sharma, D. Perez, A. Cabrera, N. Rosas and J. L. Arias, *Acta Pharmacol. Sin.*, 2008, **29**, 881–890.

82 Y. Chen, K. Yu, N. Y. Tan, R. H. Qiu, W. Liu, N. L. Luo, L. Tong, C. T. Au, Z. Q. Luo and S. F. Yin, *Eur. J. Med. Chem.*, 2014, **79**, 391–398.

83 J. Lei, Y. Liu, Y. Ou, C. T. Au, Y. Chen and S. F. Yin, *Eur. J. Med. Chem.*, 2019, **177**, 350–361.

84 R. Kant, A. K. Chandrashekar and A. K. S. Kumar, *Phosphorus, Sulfur Silicon Relat. Elem.*, 2008, **183**, 1410–1419.

85 N. Kakusawa, Y. Tobiyasu, S. Yasuike, K. Yamaguchi, H. Seki and J. Kurita, *J. Organomet. Chem.*, 2006, **691**, 2953–2968.

86 N. Tan, T. Nie, C. T. Au, D. Lan, S. Wu and B. Yi, *Tetrahedron Lett.*, 2017, **58**, 2592–2595.

87 J. Xia, R. Qiu, S. Yin, X. Zhang, S. Luo, C. T. Au, K. Xia and W. Y. Wong, *J. Organomet. Chem.*, 2010, **695**, 1487–1492.

88 C. Zhou, J. Lei, Y. Liu, C. T. Au, Y. Chen and S. F. Yin, *Appl. Organomet. Chem.*, 2020, **34**, e5881.

89 J. Lei, L. Peng, R. Qiu, Y. Liu, Y. Chen, C. T. Au and S. F. Yin, *Dalton Trans.*, 2019, **48**, 8478–8487.

90 N. Li, Q. Fan, L. Xu, R. Ma, S. Xu, J. Qiao, X. Xu, R. Guo and K. Yun, *Mol. Catal.*, 2021, **511**, 111727.

91 L. Dostal, R. Jambor, A. Ruzicka, M. Erben, R. Jirasko, E Cernoskova and J. Holecek, *Organometallics*, 2009, **28**, 2633–2636.

92 G. Strîmb, A. Pöllnitz, C. I. Raţ and C. Silvestru, *Dalton Trans.*, 2015, **44**, 9927–9942.

93 R. Qiu, Z. Meng, S. Yin, X. Song, N. Tan, Y. Zhou, K. Yu, X. Xu, S. Luo, C. T. Au and W. Y. Wong, *ChemPlusChem*, 2012, **77**, 404–410.

94 S. F. Yin, J. Maruyama, T. Yamashita and S. Shimada, *Angew. Chem. Int. Ed.*, 2008, **47**, 6590–6593.

95 X. Zhang, W. Dai, S. Yin, S. Luo and C. T. Au, *Front. Environ. Sci. Eng. China*, 2009, **3**, 32–37.

96 S. F. Yin and S. Shimada, *Chem. Commun.*, 2009, 1136–1138.

97 D. R. Kindra, I. J. Casely, M. E. Fieser, J. W. Ziller, F. Furche and W. J. Evans, *J. Am. Chem. Soc.*, 2013, **135**, 7777–7787.

98 A. Toma, C. I. Raţ, A. Silvestru, T. Rüffer, H. Lang and M. Mehring, *J. Organomet. Chem.*, 2016, **806**, 5–11.

99 X. Zhang, S. Yin, R. Qiu, J. Xia, W. Dai, Z. Yu, C. T. Au and W. Y. Wong, *J. Organomet. Chem.*, 2009, **694**, 3559–3564.

100 R. Qiu, Y. Qiu, S. Yin, X. Xu, S. Luo, C. T. Au, W. Y. Wong and S. Shimada, *Adv. Synth. Catal.*, 2010, **352**, 153–162.

101 A. M. Toma, C. I. Raţ, O. D. Pavel, C. Hardacre, T. Rüffer, H. Lang, M. Mehring, A. Silvestru and V. I. Pârvulescu, *Catal. Sci. Technol.*, 2017, **7**, 5343–5353.

102 R. Qiu, S. Yin, X. Zhang, J. Xia, X. Xu and S. Luo, *Chem. Commun.*, 2009, 4759–4761.

103 J. Ramler, I. Krummenacher and C. Lichtenberg, *Chem. - Eur. J.*, 2020, **26**, 14551–14555.

104 R. Qiu, S. Yin, X. Song, Z. Meng, Y. Qiu, N. Tan, X. Xu, S. Luo, F. R. Dai, C. T. Au and W. Y. Wong, *Dalton Trans.*, 2011, **40**, 9482–9489.

105 R. Qiu, Y. Qiu, S. Yin, X. Song, Z. Meng, X. Xu, X. Zhang, S. Luo, C. T. Au and W. Y. Wong, *Green Chem.*, 2010, **12**, 1767–1771.

106 X. Zhang, R. Qiu, N. Tan, S. Yin, J. Xia, S. Luo and C. T. Au, *Tetrahedron Lett.*, 2010, **51**, 153–156.

107 H. J. Breuning, L. K**o**nigsmann,E. Lork, M. Nema, N. Philipp, C. Silvestru, A. Soran, R. A. Varga and R. Wagner, *Dalton Trans.*, 2008, 1831–1842.

108 M. Bao, T. Hayashi and S. Shimada, *Organometallics*, 2007, **26**, 1816–1822.

109 C. W. Perkins, J. C. Martin, A. J. Arduengo, W. Lau, A. Alegría and J. K. Kochi, *J. Am. Chem. Soc.*, 1980, **102**, 7753–7759.

110 M. S. Wickleder, *Acta Crystallogr.*, 2002, **58**, i103–i104.

111 A. M. Toma, A. Pop, A. Silvestru, T. Rüffer, H. Lang and M. Mehring, *Dalton Trans.*, 2017, **46**, 3953–3962.

112 L. M. Opris, A. Silvestru, C. Silvestru, H. J. Breunig and *Dalton Trans.*, 2003, **3**, 4367–4374.

113 L. M. Opris, A. Silvestru, C. Silvestru, J. Breunig and E. Lork, *Dalton Trans.*, 2004, 3575–3585.

114 F. T. Wang, J. Najdzionek, K. L. Leneker, H. Wasserman and D. M. Braitsch, *Synth. React. Inorg. Met.-Org. Chem.*, 1978, **8**, 119–125.

115 A. Schmidpeter and H. Groeger, *Chem Ber*, 1967, **100**, 3979–3991.

116 MestReNova, Mestrelab Research S.L., Feliciano Barrera 9B – Bajo, 15706 Santiago de Compostela, Spain, https://mestrelab.com.

117 A. L. Spek, *Acta Crystallogr.*, 2009, **65**, 148–155.

118 Diamond - Crystal and Molecular Structure Visualization, Crystal Impact, Kreuzherrenstr. 102, 53227 Bonn, Germany, http://www.crystalimpact.com/diamond.

119 G. M. Sheldrick, *Acta Crystallogr.*, 2015, **71**, 3–8.

LIST OF PUBLISHED PAPERS AND CONFERENCES

Publications:

1. Lavinia Corjuc, Anca Silvestru, Cristian Silvestru, New organobismut compounds based on a tetrahydrodibenzo[c,f][1,5]azabismocine heterocyclic framework, *Revue Roumaine de Chimie*, 2023, **68(5–6)**, 209–215. DOI: 10.33224/rrch.2023.68.5-6.02

2. Lavinia Corjuc, Alexandra Pop, Emilia Licarete, Manuela Banciu, Anca Silvestru, Silver(I) complexes with diorganochalcogen ligands of type $(2\text{-}MeC_6H_4CH_2)_2E$ (E = S, Se). Synthesis, structure and antiproliferatice activity, *Inorganica Chimica Acta*, 2024, **565**, 121972. DOI: 10.1016/j.ica.2024.121972

3. Lavinia Corjuc, Levente Kiss, Anca Silvestru, Silver(I) complexes of the neutral ligands $(2\text{-}BrC_6H_4CH_2)_2E$ (E = S, Se) and $PyCH_2CH_2N(CH_2C_6H_4Br\text{-}2)_2$ (Py = pyridine). Synthesis and characterization. *Polyhedron*, *manuscript in preparation.*

Conferences:

1. Anamaria-Lavinia Corjuc, Ciprian Ionuţ Raţ, New Hypercoordinated Organoantimony(III) Compounds. Poster presentation at *International Conference of the Chemical Societies of the South-East European Countries*, 9th edition, 8-11th of May 2019, Târgoviște, Romania.

2. Anamaria-Lavinia Corjuc, Anca Silvestru, Silver Complexes with Diorganochalcogen Ligands of Type $(2\text{-}BrC_6H_4CH_2)_2E$ (E = S, Se). Oral presentation at *Young Researchers' International Conference on Chemistry and Chemical Engineering*, 3rd edition, 4-5th of June 2021, Cluj-Napoca, Romania

3. Anamaria-Lavinia Corjuc, Anca Silvestru, Silver Complexes with Diorganochalcogen Ligands of Type $(2\text{-}XC_6H_4CH_2)_2E$ (E = S, Se; X = Br, CH_3). Oral presentation at *Zilele Academice Clujene*, 21-22nd October 2021, Cluj-Napoca, Romania.

4. Anamaria-Lavinia Corjuc, Anca Silvestru, Solution behaviour and solid state structure of organoantimony(III) compounds. Poster presentation at *Conferința Națională de Chimie*, 36th edition, 4-7th of October 2022, Călimănești-Căciulata, Romania.

5. Anamaria-Lavinia Corjuc, Anca Silvestru, Structural aspects in silver complexes with diorganochalcogen ligands of type $(2\text{-}XC_6H_4CH_2)_2E$ (E = S, Se; X = Br, CH_3). Oral presentation at *Young Researchers International Conference on Chemistry and Chemical Engineering*, 4th edition,1-3rd of June 2023, Debrecen, Hungary.